Sensitivity of Iceberg Drift to Initial Size Distribution

by

Justin E. Burton
B.Sc. (Hon.), Lakehead University, 2007

A Thesis Submitted in Partial Fulfillment
of the Requirements for the Degree of

MASTER OF SCIENCE

in the School of Earth and Ocean Sciences

Supervisory Committee

Sensitivity of Iceberg Drift to Initial Size Distribution

by

Justin E. Burton
B.Sc. (Hon.), Lakehead University, 2007

Supervisory Committee

Dr. Katrin Meissner (School of Earth and Ocean Sciences)
Supervisor

Dr. Adam Monahan (School of Earth and Ocean Sciences)
Departmental Member

Dr. Andrew Weaver (School of Earth and Ocean Sciences)
Departmental Member

Abstract

Supervisory Committee
Dr. Katrin Meissner (School of Earth and Ocean Sciences)
Supervisor
Dr. Adam Monahan (School of Earth and Ocean Sciences)
Departmental Member
Dr. Andrew Weaver (School of Earth and Ocean Sciences)
Departmental Member

Historical interest in regards to icebergs have ranged from their ability to provide a freshwater source to the destructive forces they are able to impose on maritime structures. As well, recent studies have focused on the possible influences icebergs may have on the climate system. Initial investigations of the advective and deteriorative patterns of iceberg armadas under normal ablative conditions suggest that they are sensitive to their initial size distributions (Silva et al., 2006). This work extends these initial examinations further. The sensitivity of the ice and meltwater patterns to a range of initial iceberg size distributions for a collapse of the Ronne-Filchner ice shelf is investigated. A numerical iceberg model is developed, which simulates the drift and melting of iceberg populations specified in selected size categories. The model treats the population of icebergs as a continuum rather than focusing on the trajectories of individual icebergs. Oceanic and atmospheric forcing fields are provided by the University of Victoria Earth System Climate Model (UVic ESCM) and the National Centers for Environmental Prediction (NCEP) 40-year reanalysis project (Kalnay et al., 1996), respectively. Meltwater from large icebergs (with a total height of approximately 1180 m) originating from the Ronne-Filchner ice shelf reaches as far north as 58° S, compared to 63° S for small icebergs (with a total height of approximately 10 m). Also, the equivalent volume of small icebergs melts away completely within the first five years, as compared to 50 years for the large icebergs. Therefore, populations containing greater amounts of small icebergs are found to lead to a larger freshwater flux, as well as accumulate meltwater closer to the original location of the Ronne-Filchner ice shelf. These findings are important when examining the potential effect of ice shelf collapse on deep and intermediate water formation rates and associated climate feedbacks.

Table of Contents

List of Tables

List of Figures

Nomenclature

a	rate of additional ice volume due to calving [m^3s^{-1}]
A	cross-sectional area [m^2]
C	drag coefficient
f	Coriolis parameter [$rads^{-1}$]
L_a	iceberg horizontal long axis [m]
M	iceberg mass [kg]
m	rate of melting [m^3s^{-1}]
M_b	rate of basal melting (expressed in terms of length) [ms^{-1}]
M_e	rate of wave erosion (expressed in terms of length) [ms^{-1}]
M_v	rate of lateral melting (expressed in terms of length) [ms^{-1}]
p	pressure [$kgm^{-1}s^{-2}$]
ρ	density [kgm^{-3}]
S_s	sea state
T	temperature [°C]
t	time [s]
u	zonal velocity [ms^{-1}]
v	meridional velocity [ms^{-1}]
$\mathbf{v}$	velocity vector [ms^{-1}]
V	iceberg volume [m^3]
w	wind speed [ms^{-1}]
x	zonal distance [m]
y	meridional distance [m]

Subscripts

a	air
i	ice
n	maximum number of ocean layers
w	water

Acknowledgments

First and foremost, I would like to thank my supervisor, Dr. Katrin Meissner, for her contributions to this work. I would also like to extend my gratitude to Chris Avis, Dr. Alvaro Montenegro, Michael Eby, and Edward Wiebe for all of their much appreciated assistance, expertise, and patience. Additionally, thank you to the remaining members of the UVic Climate Modelling group. Also, funding provided by the Natural Sciences and Engineering Research Council of Canada, as well as the University of Victoria, is gratefully appreciated. Finally, I would like to express my appreciation to my external examiner Dr. Eddy Carmack, as well as to Dr. Adam Monahan and Dr. Andrew Weaver.

1.0 Introduction

Historically, the relationship between humans and icebergs has been marked by the danger they impose on nautical travel. An obvious example of this claim is the sinking of the Titanic in the spring of 1912. Although, in the not too distant past, there was a shift of opinion towards icebergs due to their viability as a freshwater source (Weeks and Campbell, 1973). However, this volte-face was fairly short-lived with the realization that this "source" of freshwater was not economically viable and posed a logistical challenge (Weeks and Campbell, 1973; Huppert and Turner, 1978).

The onset of offshore drilling in the early 1970s, as well as increased marine activity, throughout the high northern latitudes in the vicinity of the Grand Banks adjacent to Newfoundland, led towards increasing attention to icebergs. Great efforts have been and continue to be made in order to monitor, as well as predict, the paths of icebergs that pose a hazard (Mountain, 1980; Sodhi and El-Tahan, 1980). These efforts have had the added benefit of increasing our physical understanding of the drift and decay of these objects.

At the end of the Twentieth Century it was becoming increasingly apparent that icebergs possessed enough fresh water in large populations to affect the global climate (Broecker, 1994). This realization resulted in the development of several more contemporary numerical models to address questions regarding feedbacks between icebergs, ocean circulation and climate (Bigg et al., 1996; Gladstone et al., 2001).

The proceeding sections summarize the knowledge acquired thus far with respect to the forces that lead to an iceberg's motion and eventual decay. As well, the regional and global connections of icebergs to their environment will be discussed.

1.1 Calving

The birth of all icebergs takes place at the termini of large glacial sheets and shelves. Thus, being well informed on iceberg calving is of concern to those who wish to accurately track the ablation of major glacial masses. In fact, calving is responsible for

almost all ablation of the Antarctic Ice Sheet and roughly forty percent of the Greenland Ice Sheet (Paterson, 1994). However, regardless of this obvious importance, the physics responsible for calving is not well understood, let alone developed into any global parameterizations applicable to current numerical models (Benn et al., 2007).

Previous attempts to model the rate of calving can be grouped into two categories. Some (Pelto and Warren, 1991; Warren and Kirkbride, 2003) have tried to relate the rate of calving to variables external to the parent glacial mass, namely water depth at the terminus. Others (Van der Veen, 1996) have concentrated on variables internal to the parent glacier, focusing on the factors that control terminus position, such as stresses within the glacial mass.

A vast number of factors control calving, including: stretching associated with surface velocity gradients, force imbalances at terminal ice cliffs, undercutting by sub aqueous melting, and torques arising from buoyant forces. Due to this, solving the calving rate has led to the formulation of mainly empirical rather than physically-based functions (Brown et al., 1983; Reeh, 1968). However, the main problems associated with these functions are their regional and even temporal dependencies. These problems have led to the lack of any universal, sound representation of calving in any current numerical models. Due to these issues, contemporary iceberg models mainly assume (and underestimate) iceberg production rates from the limited observed fluxes available (Dowdeswell et al., 1992; Jacobs et al., 1992) or infer iceberg fluxes from mass balance approaches of the parent glacier (Gladstone et al., 2001).

1.2 Drift

The net sum of spatially and temporally varying external forces leads to the acceleration of an iceberg. The main forces that influence icebergs include the drags due to the relative flow of water and air past the iceberg, the Coriolis force, and the horizontal pressure gradient force. The relative magnitudes of the forces leading to iceberg motion are significantly different, with water drag being the major steering force, the second most important being the drag due to air, and the forces due to the Coriolis effect and

pressure gradients being least important but still significant. Dimensional analysis of equations (1) and (2) in section 2.2 gives evidence of these relative magnitudes.

Initial modelling studies of individual iceberg trajectories include that by Mountain (1980), as well as Sodhi and El-Tahan (1980). These studies focused upon the forces mentioned previously. Some studies also include drag forces due to the presence of sea ice (Bigg et al., 1996) and surface wave radiation (Smith, 1993). Most studies neglect forces due to sea ice and waves as a result of their small magnitude, or the lack of data available for calculation. However under circumstances of high sea ice concentrations or large sea state values these effects may become significant.

1.3 Deterioration

The deterioration of icebergs comes predominantly as a result of melting. Several other factors can be considered separate from this, such as fracturing and rollover. However, these additional processes merely increase the exposed surface area and therefore ultimately aid the melting process. Icebergs receive energy from the sun, air, and water, which leads to melting through exchange of radiation, sensible and latent heat (Robe, 1980).

Amassing knowledge with respect to the deterioration of icebergs suffers from the same problems as that associated with accumulating information on the calving of glaciers. The difficulty and danger related to gathering observational data on icebergs are understandable reasons for the lack of available information. Nevertheless, some observational studies have been carried out and have shown meltwater from icebergs to significantly alter the water properties surrounding them (e.g. Josberger and Neshyba, 1980).

Laboratory studies on the melting of icebergs have filled some but not all of the knowledge gaps left by the dearth of field studies. Most have tried to accurately simulate the salinity and temperature gradients present in the polar oceans, as well as create icebergs of similar composition and proportions as those found in nature (Huppert and Turner, 1978; Huppert and Josberger, 1980; Russell-Head, 1980). These efforts have led to empirical approximations or parameterizations that can be used in numerical models

(Løset, 1993a and 1993b; Bigg et al., 1996; Matsumoto, 1996) and only in a few cases have physically-based functions been derived (Weeks and Campbell, 1973). The model used in this study employs such empirical approximations to express the major factors contributing to iceberg deterioration.

1.4 Climate Feedbacks

On regional scales, icebergs influence their physical environment. These influences can include a change in ocean circulation, as described by Nøst and Østerhus (1998), who observed strong interruptions of Antarctic waters that form on the Berkner Bank and drain into the Filchner Trough after three giant icebergs (> 3000 km^2) became grounded on the bank in 1986. The waters of the Berkner Bank mostly remained on the western side of the icebergs having been impeded from flowing into the Filchner Trough to the east. Other examples of icebergs' influences on their physical environment include observed restrictions of pack ice movement within the Ross Sea by large fragments of the B-15 iceberg in the year 2000 (Arrigo et al., 2002). This study also reported that these restrictions subsequently led to heavier spring/summer pack ice cover than previously recorded, which in turn suppressed primary productivity in the region.

Globally, icebergs could have far reaching effects on the climate system both spatially and temporally. Meltwater can weaken or inhibit deep and intermediate water formation. It has been shown through modelling studies that deepwater formation and associated meridional heat transport are sensitive to the location and rate of freshwater forcing (Rahmstorf, 1996; Rahmstorf, 2002; Stouffer et al., 2006). As icebergs occur in polar oceans, close to deepwater formation sites, it may be important to take the trajectories of icebergs and their slow input of meltwater into account when studying climate feedbacks.

For example, during the last glacial period, large armadas of icebergs were seeded from the Laurentide Ice Sheet and other ice sheets in the surrounding area. These events have been termed Heinrich Events, named after Hartmut Heinrich who first described them (Heinrich, 1988). Some (Broecker, 1994) have attributed these events to reductions in the formation of North Atlantic Deep Water (NADW). Grimm et al. (1993) report on

the connection between episodic wet intervals in Florida prehistory and Heinrich Events. As well, Bond et al. (1993) have shown a connection between Heinrich Events and Bond cycles, where Heinrich Events occurred during the last and coldest stadial in each Bond cycle, preceding an abrupt warming event in the Northern Hemisphere. Apart from these findings, our understanding of the connection between iceberg armadas and global climate, both currently and in past climates, is still in its infancy.

1.5 Thesis Objective and Outline

The objective of this thesis is to investigate the sensitivity of drift and melt patterns of iceberg armadas to their initial size distribution. To investigate this sensitivity, a numerical model was developed based upon an approach in which the community of icebergs is viewed as a continuum rather than a system of individuals. The simulated armadas are produced by a collapse of the Ronne-Filchner ice shelf. This sensitivity could be of importance when examining the potential effect of ice shelf collapse on deep and intermediate water formation rates and associated climate feedbacks.

The topic to follow in this thesis will be a detailed description of the numerical iceberg model that was constructed and utilized for the simulations. Within this description one will find details of the various routines within the model, such as those responsible for advection and melting. After the description, a comparison between a model simulation and observations will be presented in order to gain confidence in regards to the model accuracy. Following this comparison an outline of the simulations performed, as well as the resulting data, can be found. Finally, a discussion of the results will be presented, along with the conclusions drawn from the study.

2.0 The Iceberg Model

2.1 History of Iceberg Models

Upon retrospect the evolution of iceberg modelling has followed a comprehensible pattern, when viewed from the perspective of the variations in human interest throughout the years. As mentioned in the preceding chapter, the initial motivations for studying icebergs were in the spirit of evasion, in that the primary concern was the destructive effect icebergs could impose on maritime structures. However, icebergs were briefly viewed in a positive light due to their possible ability to provide freshwater to arid nations.

Early studies of icebergs as a freshwater source mainly addressed issues regarding their life expectancies and optimal towing velocities (Weeks and Campbell, 1973). These studies stemmed from the need to bring icebergs across extensive distances into waters of much greater temperatures than polar areas. Therefore, these studies concentrated predominantly on melting rather than the free drift of icebergs.

The first iceberg drift models focused on areas where human activity encountered iceberg populations of sufficient density to be hazardous. Such a location is the north-western Atlantic Ocean, where abundant exploration for natural resources and shipping takes place in the face of one of the most active iceberg corridors on the globe. To mitigate this hazard, several numerical models were developed in order to predict iceberg paths (Mountain, 1980; Sodhi and El-Tahan, 1980). These models attempted to predict the paths of icebergs using a simple force balance that included: drags due to air and water, the Coriolis effect, and the horizontal pressure gradient force. These early models used forcing data, which was provided mainly from moored structures and ship-based instruments. However, they neglected any deterioration effects.

Later models show a shift in focus towards investigating the effects of icebergs on the climate system. Only minor differences were incorporated into the drifting schemes of these later models as compared to earlier ones, which sometimes included sea ice drag

and wave radiation (Bigg et al., 1996). However, these additional forces were often either inapplicable or of minor importance as noted by Bigg et al. (1996).

The more contemporary models were driven with more accurate and complete oceanic and atmospheric datasets. These datasets included observational information combined with output from General Circulation Models (GCMs) (Trenberth, 1989; Toggweiler, 1994). However, the major difference of these later models compared to the earlier ones was the addition of melting.

Melting was, for the most part, based upon empirical approximations (El-Tahan et al., 1987). With the incorporation of such routines into iceberg models, researchers could begin to infer the meltwater patterns produced from icebergs, with the added benefit of possibly improving the prediction of iceberg trajectories. These models were uncoupled, thus the climate feedbacks associated with the melting and drifting of icebergs could not yet be investigated. Another limitation to these trajectory-based models was their computational cost, constraining simulations to regional areas, for short durations, with small populations of icebergs (Matsumoto, 1996).

Recently, one study has fully coupled a dynamic-thermodynamic iceberg model to an Earth Model of Intermediate Complexity (EMIC) (Jongma et al. 2009). Jongma et al. (2009) investigated the effect of dynamic-thermodynamic icebergs on deepwater formation in the Southern Ocean, as compared to the standard parameterization of prescribed freshwater due to iceberg "calving", in which meltwater is applied over predefined ocean areas adjacent to the coast. Results from the study show the dynamic-thermodynamic icebergs to increase Antarctic Bottom Water (AABW) formation by 10%, as compared to the parameterization. The iceberg model used in the study tracks the trajectories of individual icebergs and is therefore computationally limited to a small number of icebergs per simulation.

2.2 Model Description

When viewed on ocean basin scales over seasonal, or annual, time periods, communities of icebergs behave much like a fluid spreading out in lobes, dispersing and diffusing. If one's concern is not the exact trajectories of individual icebergs but the

overall effects of armadas on the climate system then the continuum approach is ideal. Initial modelling attempts to characterize icebergs in such a fashion were completed by La Prairie (1999) and subsequently published in Clarke and La Prairie (2001).

The experiments by La Prairie (1999) were applied specifically to palaeoclimate studies of Heinrich Events in the North Atlantic during the last glacial period. La Prairie (1999) simulated iceberg distributions, with associated meltwater and sedimentation patterns, and compared these to sediment records. Due to the application of the continuum approach, La Prairie (1999) was able to perform millennial-scale integrations. Here, I follow the theoretical approach of Clarke and La Prairie (2001) to develop a computationally efficient iceberg model.

2.2.1 Advection

The advection of iceberg volume within the model is accomplished in two routines. First, the iceberg velocity field is calculated from the specified equations of motion (shown in Cartesian form in equations (1) and (2)). The equations contain the major factors that drive the movement of an iceberg, namely: drags due to air and water, the Coriolis force, and the horizontal pressure gradient force.

$$\frac{du}{dt} = f\left(v - v_G\right) + \frac{1}{2M}\rho_a C_a A_a \left|\mathbf{v}_a - \mathbf{v}\right|\left(u_a - u\right) + \frac{C_w \rho_w}{2M}\sum_{i=1}^{n}\left(A_{w_i}\left|\mathbf{v}_{w_i} - \mathbf{v}\right|\left(u_{w_i} - u\right)\right) \quad (1)$$

$$\frac{dv}{dt} = -f\left(u - u_G\right) + \frac{1}{2M}\rho_a C_a A_a \left|\mathbf{v}_a - \mathbf{v}\right|\left(v_a - v\right) + \frac{C_w \rho_w}{2M}\sum_{i=1}^{n}\left(A_{w_i}\left|\mathbf{v}_{w_i} - \mathbf{v}\right|\left(v_{w_i} - v\right)\right) \quad (2)$$

For the above equations u and v are the iceberg zonal and meridional velocities, respectively, with t representing time. The density is represented by ρ. u_G and v_G are the geostrophic components of the zonal and meridional ocean velocities, respectively. The Coriolis parameter is specified as f, the iceberg mass as M, the drag coefficient as C, the cross-sectional area as A, n is the maximum ocean layer, and subscripts a and w represent values corresponding to the atmosphere and ocean, respectively. The velocity vector is represented as $\mathbf{v}$ and velocity terms lacking a subscript indicate values pertaining to ice.

All icebergs within the model are specified to be cylinders with a height to diameter ratio of one, which corresponds fairly well to the height to diameter ratio of 1.5

for North Atlantic icebergs (Robe, 1980). The cylindrical geometry was chosen to allow the drag portions of the above equations to remain constant regardless of the prevailing flow direction. The drag coefficient C was set to 1.5 for both air and water (Mountain, 1980). The University of Victoria Earth System Climate Model (UVic ESCM) grid is utilized for the iceberg model, having a resolution of 1.8° meridionally by 3.6° zonally. For more information regarding the UVic ESCM please refer to Weaver et al. (2001).

Equation (3) describes the conservation of mass and is discretized in the model using an upstream method, explicit in time. The iceberg velocity field values are specified at the corners of the advection grid, giving a staggered orientation (Kundu and Cohen, 2004). In the below expression, V characterizes the iceberg volume, $\mathbf{v}$ the iceberg velocity field, a any addition due to glacial calving, and m any losses due to melting of icebergs. Incompressibility is assumed, allowing the below form of the advection equation to be stated. The below expression is integrated over space, time, as well as size categories in the iceberg model.

$$\frac{\partial V}{\partial t} + \nabla \cdot (\mathbf{v} V) = a - m \tag{3}$$

2.2.2 Melting

The effects due to wave erosion, basal convection, and buoyant convection, characterize the melting of icebergs within the model. Erosion of icebergs due to the force of waves is the most important of these three mechanisms, leading to more than 80% of the overall corrosion of icebergs (El-Tahan et al., 1987). It is described, in m of length/day, by the following empirical functions:

(Wave Erosion) $$M_e = \frac{1}{18}(T + 2) S_s \tag{4}$$

(Sea State) $$S_s = \left(\frac{w}{0.836} \right)^{2/3} \tag{5}$$

The parameterization of wave erosion (equation (4)) is taken from Gladstone et al. (2001), in terms of T, the sea surface temperature in degrees Celsius and S_s, the sea state. The sea state is calculated via the empirical relation given above (equation (5)), where w represents the wind speed at 10 m in m/s according to the marine Beaufort scale (Beer, 1997).

Basal convection results from the relative velocity of the iceberg base to that of the ambient seawater, in combination with temperature and salinity gradients at the base. Basal convection is found to be the second most important corrosive force, leading to approximately 16% of the overall deterioration (El-Tahan et al., 1987). As this form of convective heat transfer depends on the relative velocity of the iceberg, it is sometimes referred to as "forced convection". This differs from "free convection", which depends solely upon the temperature gradient between the ice and water.

The basal convection expression was first adapted by Weeks and Campbell (1973) from the original derivation of Eckart and Drake (1959) to be applicable to iceberg freshwater harvesting studies. It was then modified by Bigg et al. (1997) for studying the drift and melt of icebergs:

(Basal Convection) $$M_b = 0.58\left|\mathbf{v}_w - \mathbf{v}_i\right|^{0.8} \frac{T_w - T_i}{L_a^{0.2}} \qquad (6)$$

Velocity in m/s is represented by **v**, with subscripts w and i specifying values relative to the water and ice, respectively. T is the temperature in degrees Celsius, and L_a the diameter of the iceberg in m. The temperatures, T_i and T_w, are set to the equilibrium iceberg skin temperature (T_i = - 4° C), as found in the high resolution melting study of Løset (1993a and b), and the sea surface temperature simulated by the UVic ESCM (Weaver et al., 2001).

The third manner by which icebergs effectively melt, buoyant convection, is due to the interaction of the sidewalls of the iceberg with the surrounding seawater. This form of melting can be thought of as "free convection" and is found to only be responsible for roughly 2% of the deterioration of icebergs (El-Tahan et al., 1987). An empirical relationship for the melt due to buoyant convection was first developed by El-Tahan et al.

(1987), with the only variable being the ocean temperature in degrees Celsius. The buoyant convection function used in this model was subsequently modified by Bigg et al. (1997):

$$\text{(Buoyant Convection)} \qquad M_v = 7.62\times10^{-3}T_w + 1.29\times10^{-3}T_w^2 \tag{7}$$

Here we approximate T_w as the sea surface temperature for simplicity. This approximation makes little difference in the overall deterioration of the iceberg, as melting due to buoyant convection is an order of magnitude smaller than other melting functions.

The above deterioration factors operate on different portions of the cylinders. The wave erosion and buoyant convection act to reduce the diameter of the cylinders, whereas the basal convection acts to shorten the cylinders. However, we adjust the mass transfer so that the height to diameter ratio of the cylinders remains constant throughout integration.

Effects due to solar and long wave radiation, as well as sensible and latent heat exchanges with the atmosphere are neglected given that they only account for the remaining small percentage (~2%) of overall corrosion (El-Tahan et al., 1987).

2.2.3 Size Categories

Icebergs of differing volumes demonstrate different behaviour in response to advective and deteriorative forces. The study of Clarke and La Prairie (2001) accounts for this by taking different size categories into consideration. The present study takes the same insight and places iceberg volume in eight pre-defined size categories. Each category still retains the height to diameter ratio of one.

Size categories in the present model were chosen according to the UVic ESCM ocean layers (Figure 1), because the major force acting on icebergs is water drag. The ratio of the submerged height of the iceberg compared to the total height was calculated based upon an average density of 850 kg/m^3 for Antarctic ice shelf icebergs, as compared

to Arctic icebergs with an average density of 895 kg/m^3, and an average seawater density of 1025 kg/m^3 (Table 1) (Weeks and Campbell, 1973).

Figure 1 shows the iceberg velocity (blue line) as a function of submerged height for given wind and ocean velocity fields. Also shown are the velocities of each pre-defined size category (in red) and the depth of each ocean layer (in black). Annual mean ocean and wind velocities from the UVic ESCM and NCEP, respectively, were utilized in order to calculate the ice velocities. The velocities shown in Figure 1 are an average calculated from ten different sites in the North Atlantic (Figure 2).

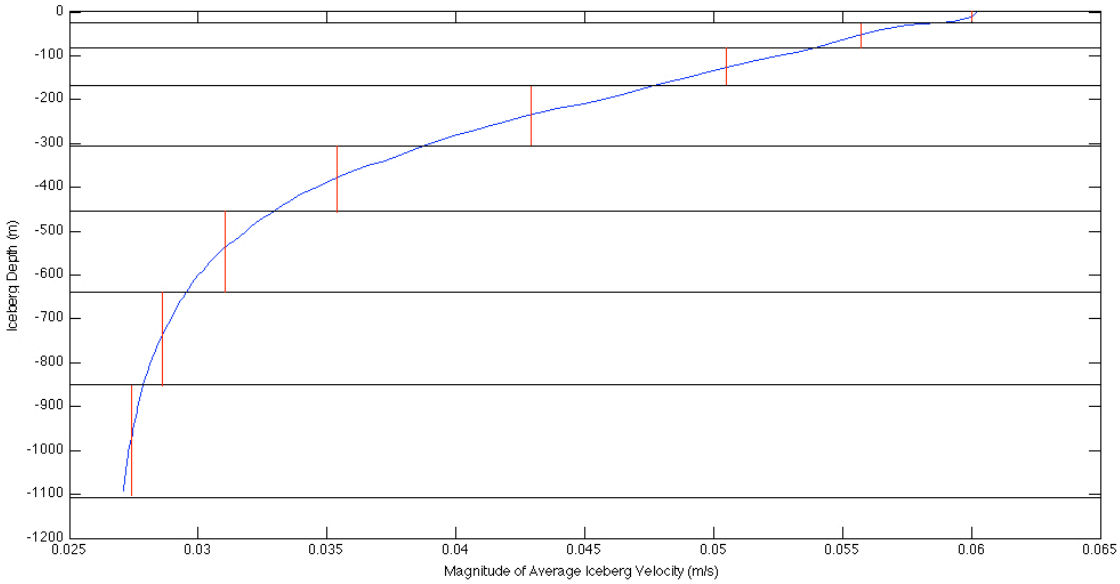

Figure 1: Annual mean iceberg velocity as a function of submerged height. The blue line shows iceberg velocity, the red line shows velocities for each size category and black lines represent the depths of the UVic ESCM ocean layers.

Table 1: Iceberg size category characteristics

Size Category	Depth Below Sea Level (m)	Total Height (H) (m)
1	Open Water	Open Water
2	9	11
3	50	60
4	130	157
5	240	289
6	380	458
7	550	663
8	750	904
9	980	1181

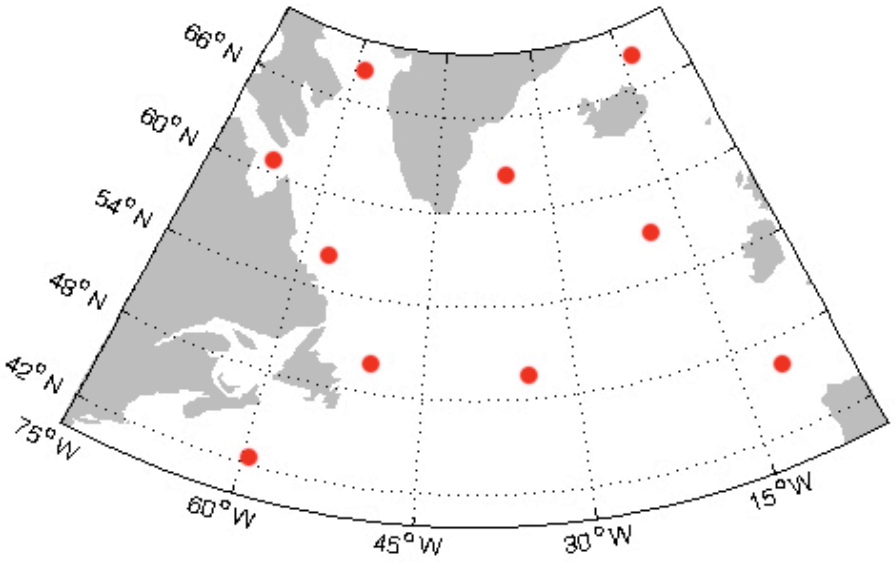

Figure 2: Location of sites throughout the North Atlantic (red circles) used for the calculation of average iceberg velocity in Figure 1.

During simulations the change in size is unidirectional, in that icebergs are only transferred from larger categories to smaller ones as a result of melting. Melting acts upon the total iceberg volume within a particular size category within the grid cell in question. This melting results in two ultimate outcomes: some amount of the volume is converted into meltwater and some iceberg volume is transferred to the lower category, with the lowest category representing water only.

2.3 Comparison to Observations

For the purposes of avoiding catastrophes in offshore resource exploration and maritime travel, Environment Canada provides a biweekly report of iceberg distributions. These observations are focused on an area of the north-western Atlantic Ocean, which encompasses a portion of the trans-Atlantic marine shipping lanes and numerous offshore drilling structures. The observational reports span the time period from approximately mid-February to mid-July of each year. Data for the reports are gathered from numerous sources including ships, merchant and Coast Guard, satellites (National Ice Center (NIC) and C-CORE), as well as aircraft (predominantly the International Ice Patrol (IIP)). These various forms of data are then merged into a single document, which is subsequently provided to the public (USCG, 2008). The Canadian and US Coast Guards maintain an active working relationship, along with other private interests mentioned (merchant ships and satellite providers), to accomplish this task. Much of this effort came as a result of the 1912 sinking of the Titanic, upon which time the IIP was formed under the US Coast Guard (USCG, 2008).

The iceberg model simulation was compared to the 2008 biweekly iceberg observations provided by Environment Canada (Environment Canada, 2008). These observations were chosen, instead of more remote areas such as Antarctica, due to the density of observations available. This fact should be noted as the iceberg model will be used later on for simulations in the Southern Hemisphere (Chapter 3). The decreased height to length ratio of icebergs (tabular icebergs) and the high seasonality of sea ice in the Southern Hemisphere encompass some of the main differences of iceberg characteristics and environmental conditions between the two areas.

Although the Environment Canada data are the best available source, they are still limited because icebergs are only observed over a relatively small area of responsibility (AOR, white area in Figure 3), which is far from calving sources, and because a continuous time series is not available. As well, iceberg sizes are not reported. I therefore chose to simulate the drift of the most frequently encountered size category based on the frequency distribution provided by the IIP for an average ice season (Table 2). The most frequently encountered size categories are equivalent to small and medium icebergs

under international classification, and encompass icebergs with total heights of 5 - 15 m and 16 – 45 m and approximate height to diameter ratios of 1:1.5 (USCG, 2008). Although small icebergs are as frequent as medium icebergs (Table 2), an iceberg size distribution for the 2008 iceberg season is not available, as previously mentioned. Therefore, the numbers of icebergs within the observations were assumed to represent one size category, that being medium icebergs (approximately equivalent to model size category 3).

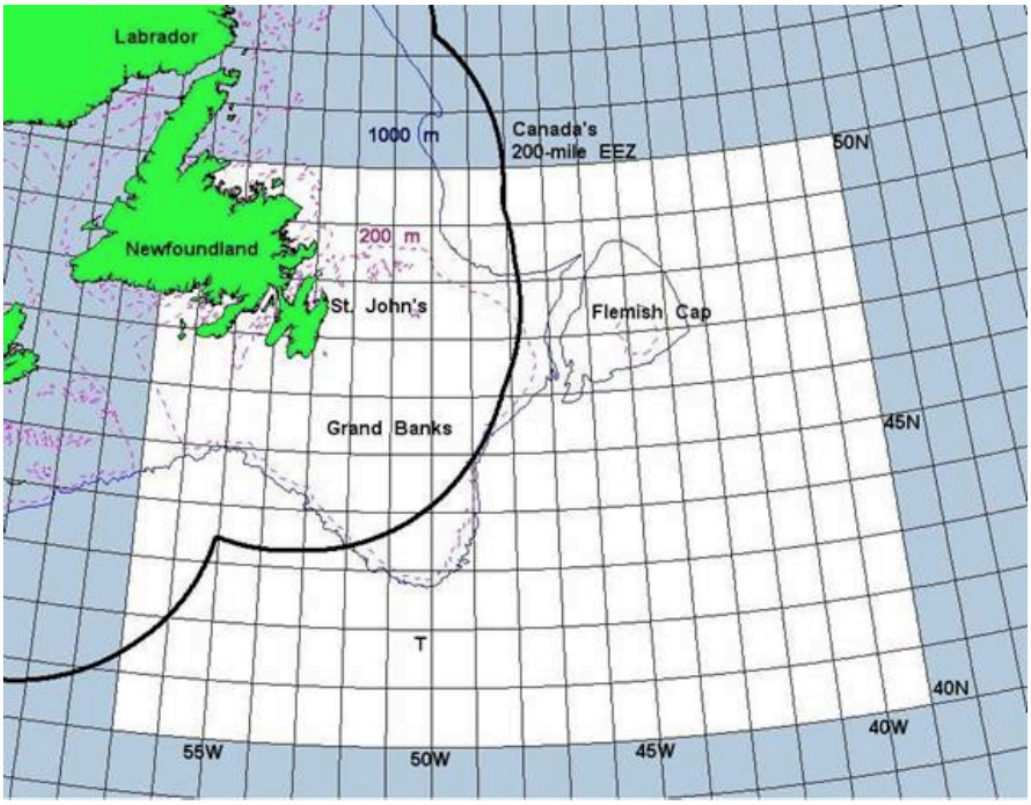

Figure 3: Area of responsibility (white area) for the IIP (USCG, 2008)

Table 2: Size distribution of icebergs within the IIP AOR (USCG, 2008)

SIZE CATEGORY	Total Height (m)	% OF TOTAL NUMBER
Growler	< 1	5.6
Bergy Bit	1 – 5	-
Small	5 – 15	15.3
Medium	16 – 45	15.3
Large	46 – 75	12.5
Very Large	> 75	2.8
General (Size Unknown)	-	48.5

Icebergs with a uniform height of 60 m and a height to diameter ratio of 1:1 were seeded from four source grid cells directly adjacent to the coasts of Labrador and Newfoundland. The calving sources were constrained by the Environment Canada observations for both timing and amount.

The atmospheric forcing field was provided by the National Centers for Environmental Prediction (NCEP) reanalysis model and the oceanic forcing fields were provided by the Estimating the Circulation and Climate of the Ocean (ECCO) reanalysis project. These sources of forcing data are considered some of the most robust, due to the simulations being continuously calibrated with available observations. The retrieved datasets, which span the same time period as the iceberg observations, were interpolated to the iceberg model grid and composed into monthly averages.

The 2008 iceberg observations can be seen below (Figure 4). The two available variables for comparison with the Environment Canada iceberg observations are the number of icebergs per 1° square of ocean surface and the Limit of All Known Ice (LAKI), represented by the solid magenta contour in the Figure 4 observations. This limit is taken to be the contour that corresponds to one size category 3 iceberg in the model (magenta contour in the Figure 4 simulations). Contours throughout the model simulations are in terms of the number of medium icebergs per 1° square area.

Comparing observations to the model simulations, the importance of sea ice as a driving force becomes obvious (Schodlok et al., 2006). It was reported in Schodlok et al. (2006) that concentrations of sea ice above approximately 86% lead to coherent drift tracks between icebergs and sea ice. Sea ice concentrations of 86% or greater are

observed over most iceberg seasons throughout the area adjacent to the Labrador coast and over the Grand Banks (the stippled magenta contour in the Figure 4 observations marks the extent of sea ice). The distribution of observed icebergs for snapshots taken between April 15 and June 15 show a southward extent that cannot be simulated by the model. This may be due to the lack of a sea ice component and its ability to move icebergs. Also, iceberg concentrations observed throughout the latter half of the observational period could not be reproduced. This may be due to the lack of information regarding iceberg size distribution and the fact that observations are taken far from calving sources.

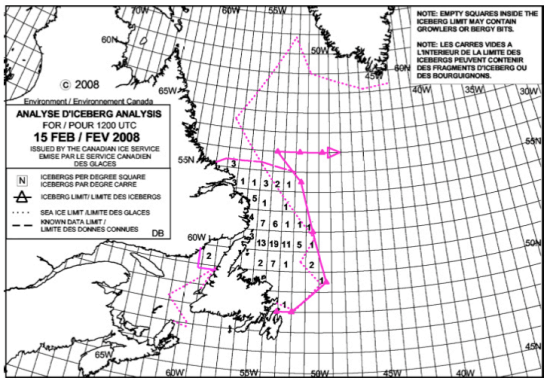
© 2008
Environment / Environnement Canada
ANALYSE D'ICEBERG ANALYSIS
FOR / POUR 1200 UTC
15 FEB / FEV 2008
ISSUED BY THE CANADIAN ICE SERVICE
EMISE PAR LE SERVICE CANADIEN DES GLACES
ICEBERGS PER DEGREE SQUARE
ICEBERGS PAR DEGRE CARRE
ICEBERG LIMIT/ LIMITE DES ICEBERGS
SEA ICE LIMIT /LIMITE DES GLACES
KNOWN DATA LIMIT / LIMITE DES DONNES CONNUES
DB
NOTE: EMPTY SQUARES INSIDE THE ICEBERG LIMIT MAY CONTAIN GROWLERS OR BERGY BITS.
NOTE: LES CARRES VIDES A L'INTERIEUR DE LA LIMITE DES ICEBERGS PEUVENT CONTENIR DES FRAGMENTS D'ICEBERG OU DES BOURGUIGNONS.

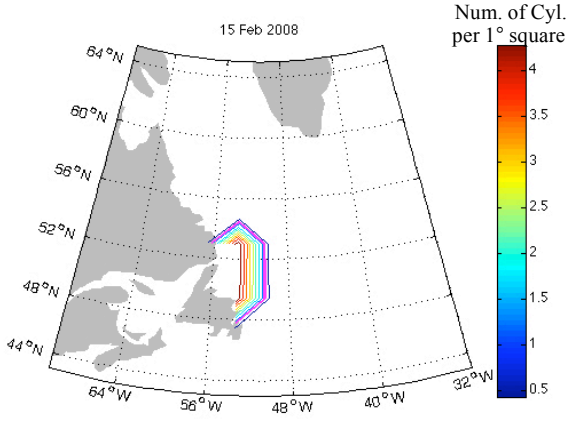
15 Feb 2008
Num. of Cyl. per 1° square

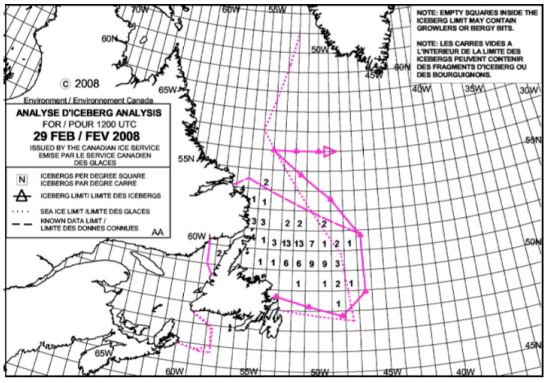
© 2008
Environment / Environnement Canada
ANALYSE D'ICEBERG ANALYSIS
FOR / POUR 1200 UTC
29 FEB / FEV 2008
ISSUED BY THE CANADIAN ICE SERVICE
EMISE PAR LE SERVICE CANADIEN DES GLACES
ICEBERGS PER DEGREE SQUARE
ICEBERGS PAR DEGRE CARRE
ICEBERG LIMIT/ LIMITE DES ICEBERGS
SEA ICE LIMIT /LIMITE DES GLACES
KNOWN DATA LIMIT / LIMITE DES DONNES CONNUES
AA
NOTE: EMPTY SQUARES INSIDE THE ICEBERG LIMIT MAY CONTAIN GROWLERS OR BERGY BITS.
NOTE: LES CARRES VIDES A L'INTERIEUR DE LA LIMITE DES ICEBERGS PEUVENT CONTENIR DES FRAGMENTS D'ICEBERG OU DES BOURGUIGNONS.

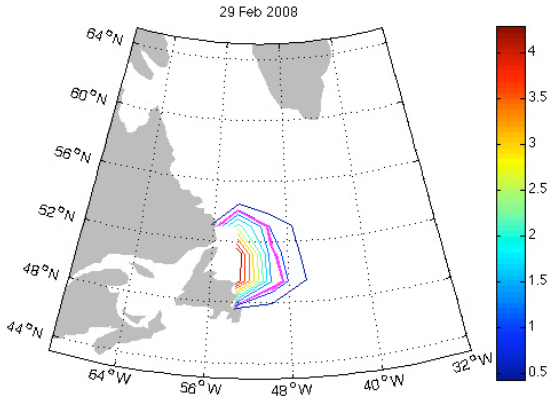
29 Feb 2008

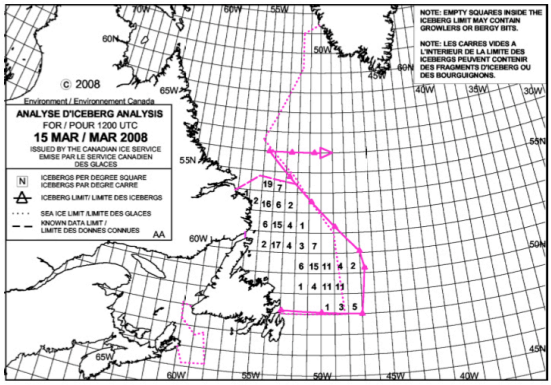
© 2008
Environment / Environnement Canada
ANALYSE D'ICEBERG ANALYSIS
FOR / POUR 1200 UTC
15 MAR / MAR 2008
ISSUED BY THE CANADIAN ICE SERVICE
EMISE PAR LE SERVICE CANADIEN DES GLACES
ICEBERGS PER DEGREE SQUARE
ICEBERGS PAR DEGRE CARRE
ICEBERG LIMIT/ LIMITE DES ICEBERGS
SEA ICE LIMIT /LIMITE DES GLACES
KNOWN DATA LIMIT / LIMITE DES DONNES CONNUES
AA
NOTE: EMPTY SQUARES INSIDE THE ICEBERG LIMIT MAY CONTAIN GROWLERS OR BERGY BITS.
NOTE: LES CARRES VIDES A L'INTERIEUR DE LA LIMITE DES ICEBERGS PEUVENT CONTENIR DES FRAGMENTS D'ICEBERG OU DES BOURGUIGNONS.

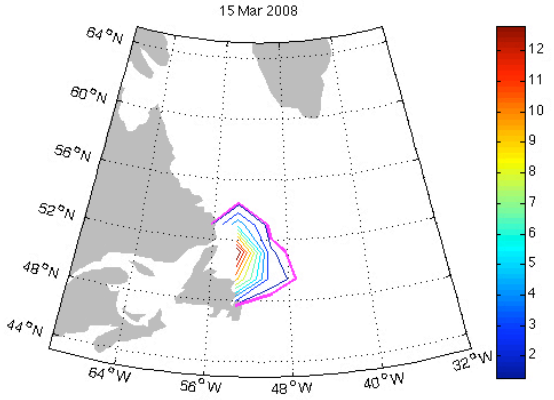
15 Mar 2008

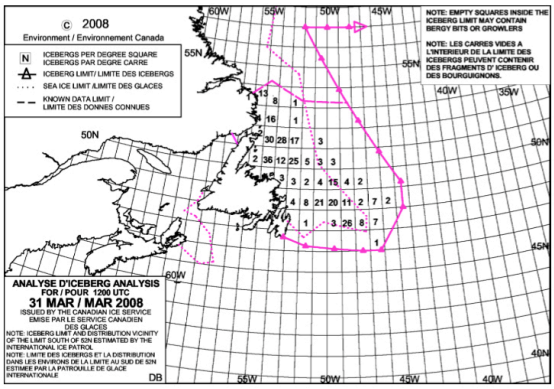
© 2008
Environment / Environnement Canada
ANALYSE D'ICEBERG ANALYSIS
FOR / POUR 1200 UTC
31 MAR / MAR 2008
ISSUED BY THE CANADIAN ICE SERVICE
EMISE PAR LE SERVICE CANADIEN DES GLACES
ICEBERGS PER DEGREE SQUARE
ICEBERGS PAR DEGRE CARRE
ICEBERG LIMIT/ LIMITE DES ICEBERGS
SEA ICE LIMIT /LIMITE DES GLACES
KNOWN DATA LIMIT / LIMITE DES DONNES CONNUES
NOTE: ICEBERG LIMIT AND DISTRIBUTION VICINITY OF THE LIMIT SOUTH OF 52N ESTIMATED BY THE INTERNATIONAL ICE PATROL
NOTE: LIMITE DES ICEBERGS ET LA DISTRIBUTION DANS LES ENVIRONS DE LA LIMITE AU SUD DE 52N ESTIMEE PAR LA PATROUILLE DE GLACE INTERNATIONALE
DB
NOTE: EMPTY SQUARES INSIDE THE ICEBERG LIMIT MAY CONTAIN BERGY BITS OR GROWLERS
NOTE: LES CARRES VIDES A L'INTERIEUR DE LA LIMITE DES ICEBERGS PEUVENT CONTENIR DES FRAGMENTS D' ICEBERG OU DES BOURGUIGNONS.

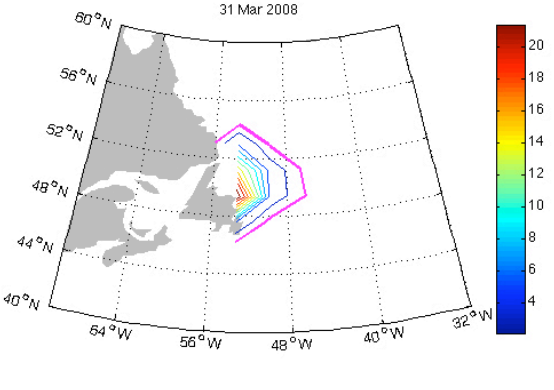
31 Mar 2008

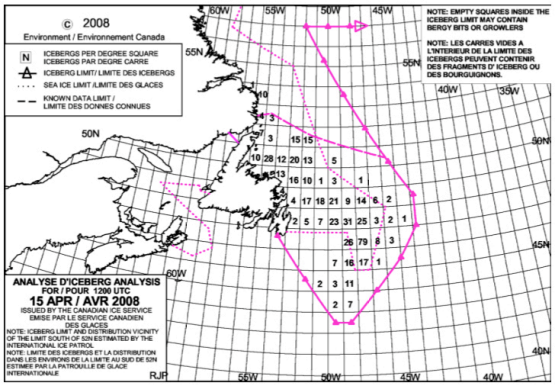
© 2008
Environment / Environnement Canada
ANALYSE D'ICEBERG ANALYSIS
FOR / POUR 1200 UTC
15 APR / AVR 2008
ISSUED BY THE CANADIAN ICE SERVICE
EMISE PAR LE SERVICE CANADIEN DES GLACES
RJR

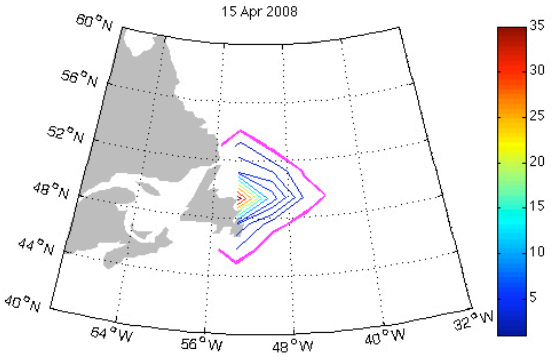
15 Apr 2008

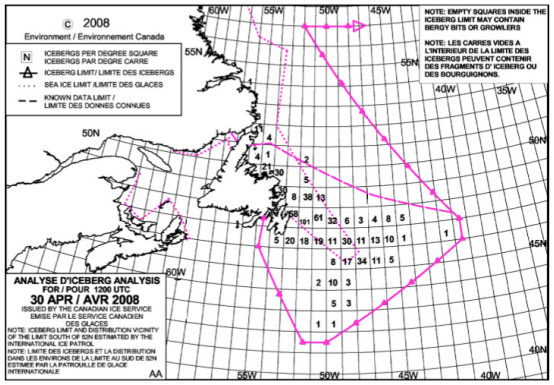
© 2008
Environment / Environnement Canada
ANALYSE D'ICEBERG ANALYSIS
FOR / POUR 1200 UTC
30 APR / AVR 2008
ISSUED BY THE CANADIAN ICE SERVICE
EMISE PAR LE SERVICE CANADIEN DES GLACES
AA

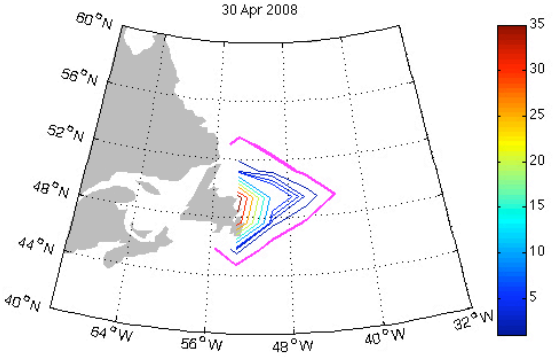
30 Apr 2008

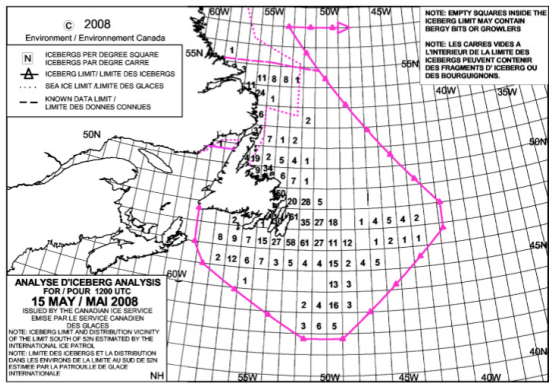
© 2008
Environment / Environnement Canada
ANALYSE D'ICEBERG ANALYSIS
FOR / POUR 1200 UTC
15 MAY / MAI 2008
ISSUED BY THE CANADIAN ICE SERVICE
EMISE PAR LE SERVICE CANADIEN DES GLACES
NH

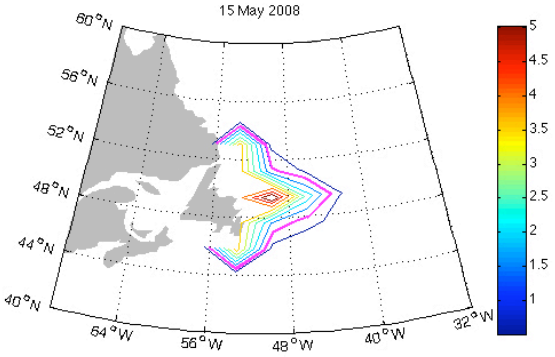
15 May 2008

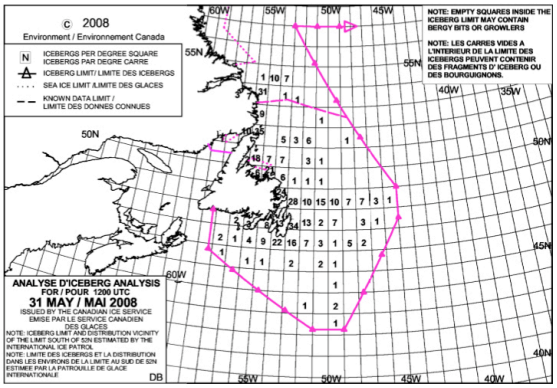
© 2008
Environment / Environnement Canada
ANALYSE D'ICEBERG ANALYSIS
FOR / POUR 1200 UTC
31 MAY / MAI 2008
ISSUED BY THE CANADIAN ICE SERVICE
EMISE PAR LE SERVICE CANADIEN DES GLACES
DB

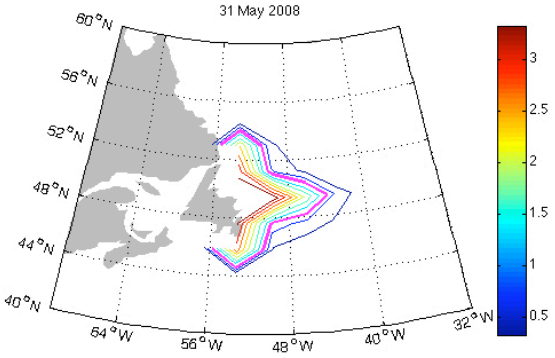
31 May 2008

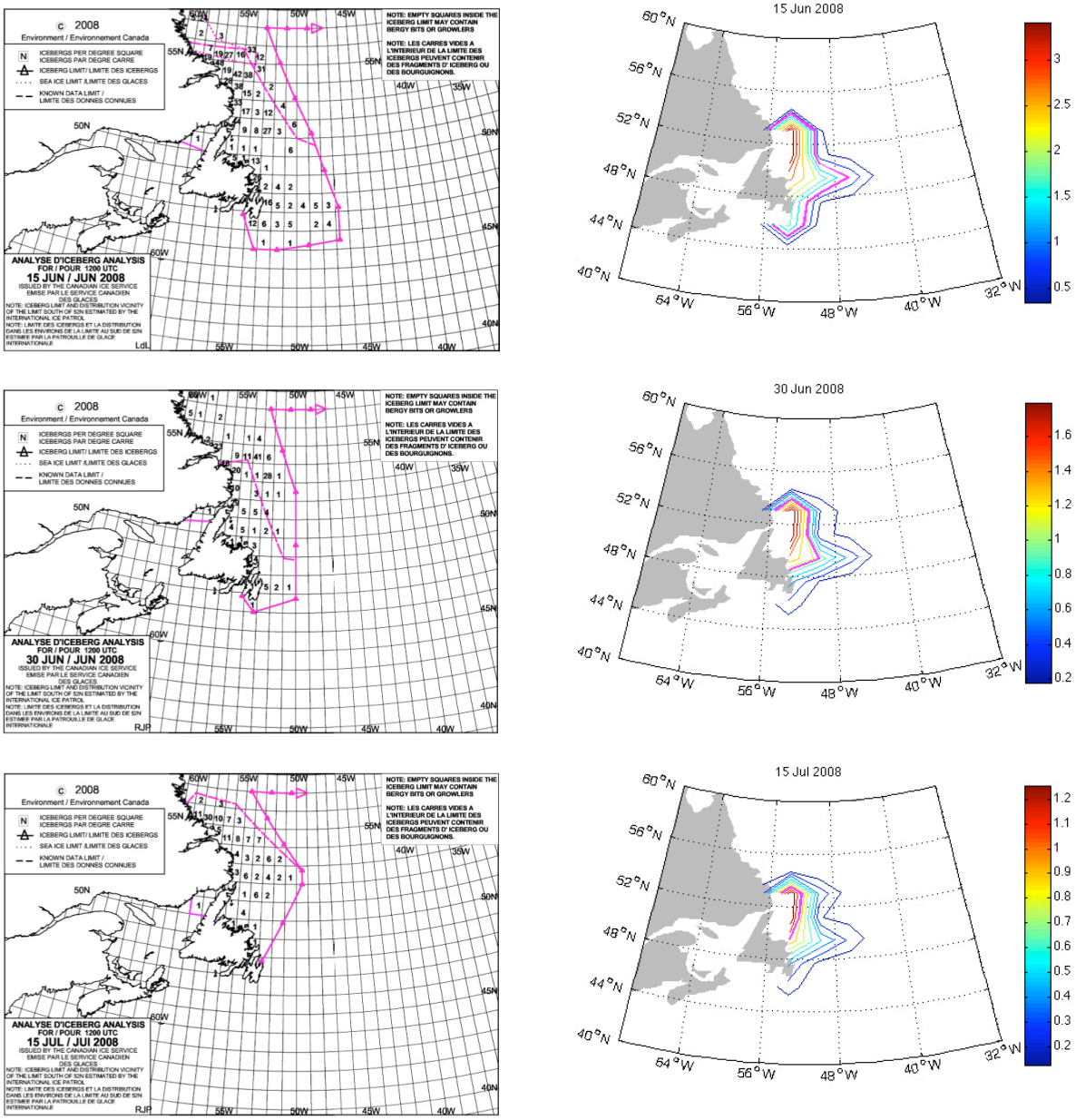

Figure 4: Comparison between 2008 Environment Canada iceberg observations (left column, in number of icebergs per degree square) and simulated iceberg distributions (right column). Model simulation contours are in terms of the number of medium icebergs (size category 3) per 1° square area. The magenta contour throughout the model simulations represents one medium iceberg.

3.0 The Impact of Initial Size Distribution on Drift and Meltwater Pattern

3.1 Background

Most observed iceberg size frequency distributions have exhibited a log-normal pattern, viewed from both Greenlandic and Antarctic sources (Morgan and Budd, 1978; Weeks and Mellor, 1978; Dowdeswell et al., 1992). However this distributive pattern occurs during typical ablative periods. If more anomalous calving episodes were to occur, which could result from the effects of rapid shelf destruction, size distributions that stray from the norm may be observed. An example is the 2002 collapse of the Larsen B ice shelf, which produced numerous "giant" icebergs (> 18.5 km in length) (NSIDC, 2009).

Studies regarding the varying effects of iceberg drift and deterioration, relative to their size distributions, are currently sparse. Reasons behind this lack of information are observational limitations and computational constraints. However, what studies do exist emphasize that varying size distributions lead to substantially varying outcomes. Due to most of the great ice shelves on the globe being located around the continent of Antarctica, the vast majority of these studies are focused around this area (BAS, 2009).

For example, Gladstone et al. (2001) examined the distribution of iceberg trajectories and associated meltwater patterns of small tabular icebergs within the Southern Ocean with an uncoupled, dynamic-thermodynamic iceberg model. This study was restricted to tabular icebergs of no greater length than 2.2 km (with an average thickness of 0.25 km), which are considered small by Antarctic standards. They found the Coriolis force an important factor for the entrainment of icebergs adjacent to the Antarctic coast, for icebergs travelling westward in the Antarctic coastal current. As well, it was found that the production of meltwater was comparable in magnitude to precipitation minus evaporation in many coastal regions.

On the other hand, Silva et al. (2006) simulated the meltwater distributions of "giant" icebergs (> 18.5 km in length and an average thickness of 0.25 km) combining a thermodynamic iceberg model with observed drift tracks. The difference between the

results of Silva et al. (2006) and those of Gladstone et al. (2001) were considerable. It was estimated that 35% of the giant icebergs' mass is exported north of 63° S compared to only 3% of the smaller icebergs' initial mass, although the larger icebergs spend more time of the earlier part of their history near the coast. This effect can most likely be attributed to the fact that larger icebergs are more ocean-driven and smaller icebergs are more wind-driven. Considering the dominant ocean circulation (Figure 7 to Figure 9) around the Antarctic continent, as well as the dominant wind circulation (Figure 10), the results of Silva et al. (2006) are understandable.

It seems that the initial size of an iceberg has an important influence on its drift and melting. This fact is the motivation for the present inquiry: the investigation of ice volume and meltwater patterns caused by a collapse of the Ronne-Filchner ice shelf depending on the initial size variation.

Throughout the past 50 years, an estimated 87% of ice shelf termini throughout the Antarctic Peninsula have retreated (Cook et al., 2005). Also, marine sediment cores show that shelves in the region have likely not reached a comparable minimum extent for at least the last 10,000 years (Domack et al., 2005) and certainly not for the last 1,000 years (Pudsey et al., 2006). Assessments on the future stability of ice shelves throughout the area suggest that the waning of these great ice masses seems inevitable in the face of global warming (BAS, 2009). Furthermore, the largest ice shelf on the globe in terms of volume, the Ronne-Filchner ice shelf ($\sim 2.1 \times 10^{14}$ m^3), is located directly adjacent to the Antarctic Peninsula. These facts in combination with the results of Silva et al. (2006) (see above) prompt the current study to investigate the possible variability in ice and subsequent meltwater patterns due to differing initial size distributions for a collapsing Ronne-Filchner shelf (Figure 5 and Figure 6).

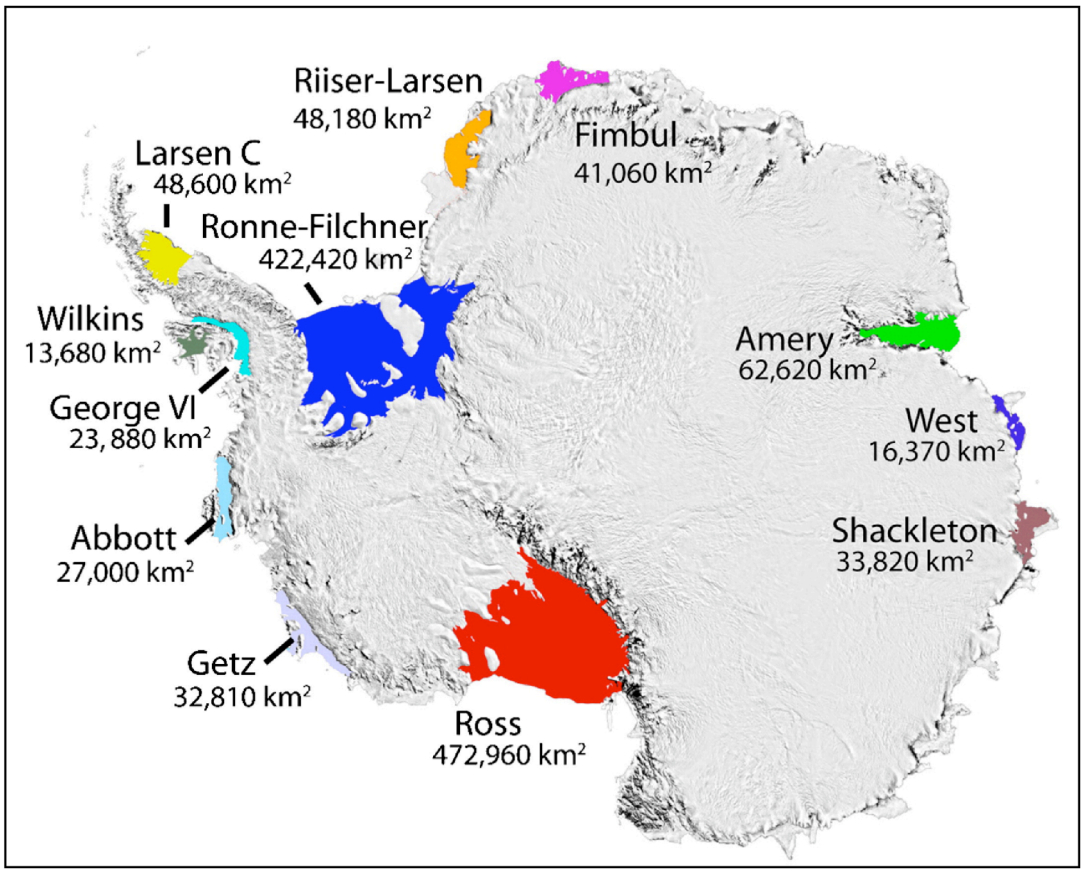

Figure 5: Major Antarctic ice shelves (2007) (NSIDC, 2009)

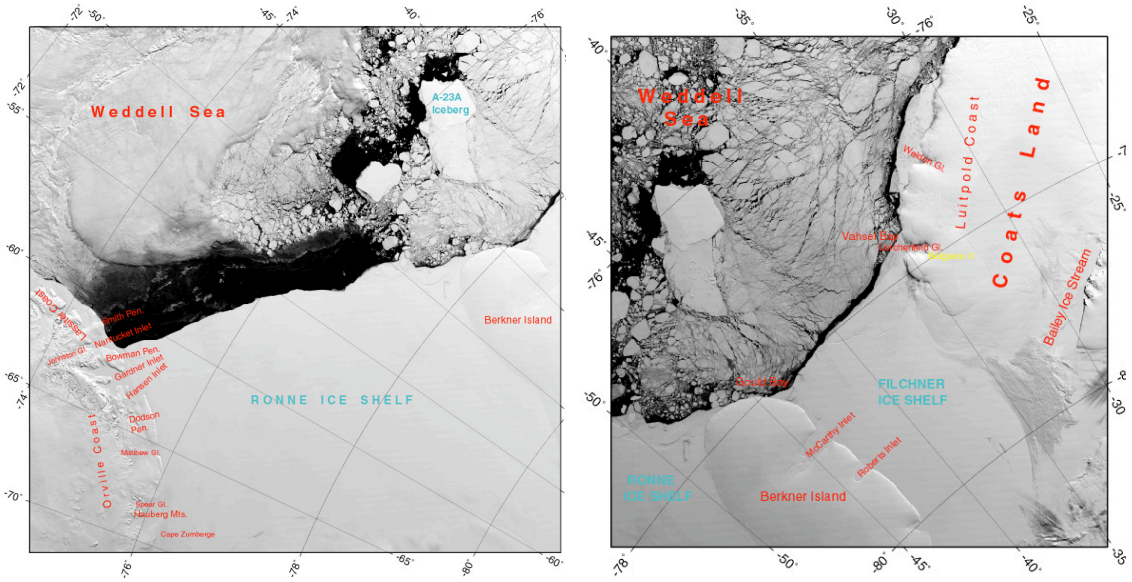

Figure 6: Ronne-Filchner ice shelf (2002) (NSIDC, 2009)

3.2 Experimental Setup

The study utilizes the dynamic-thermodynamic iceberg model, as described in section 2.2, along with ocean and atmosphere forcing fields provided by the UVic ESCM (Figure 7 through Figure 9) and NCEP (Figure 10) (Kalnay et al., 1996), respectively. Forcing data for all scenarios include monthly averaged, pre-industrial ocean currents and sea surface temperatures, along with present day winds. All iceberg initializations were based upon an estimate of the Ronne-Filchner ice shelf containing approximately 2.1×10^{14} m^3 of ice. This volume is based upon an estimation of the Ronne-Filchner ice shelf having an approximate surface area of 420,000 km^2 and an average thickness of 0.5 km (NSIDC, 2009).

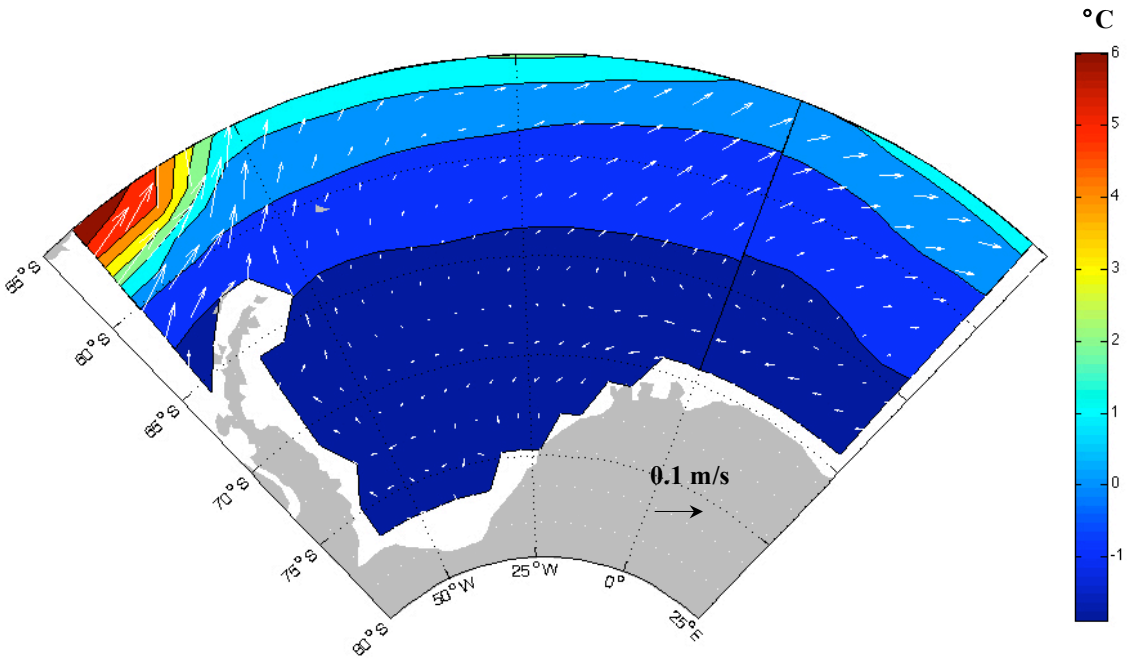

Figure 7: Annually averaged UVic ESCM surface ocean velocities and sea surface temperatures

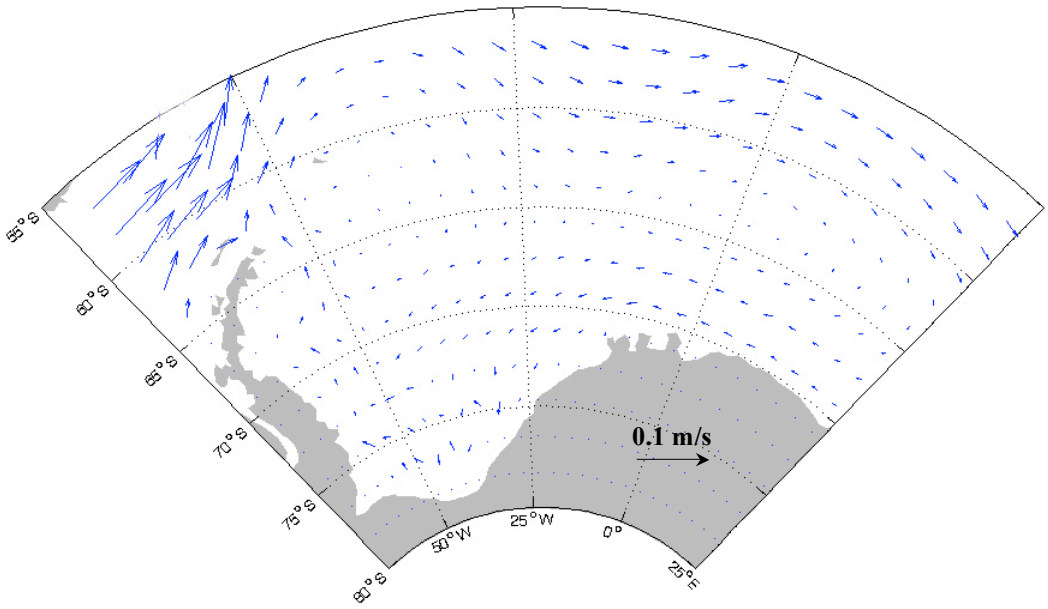

Figure 8: Annually averaged UVic ESCM ocean velocities at 240.0 m depth

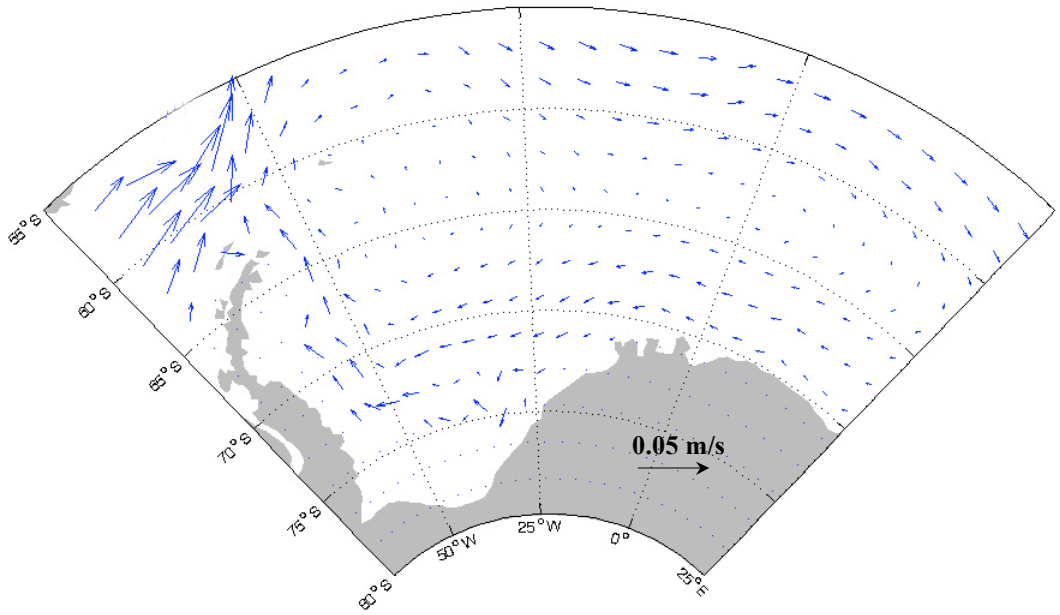

Figure 9: Annually averaged UVic ESCM ocean velocities at 980.0 m depth

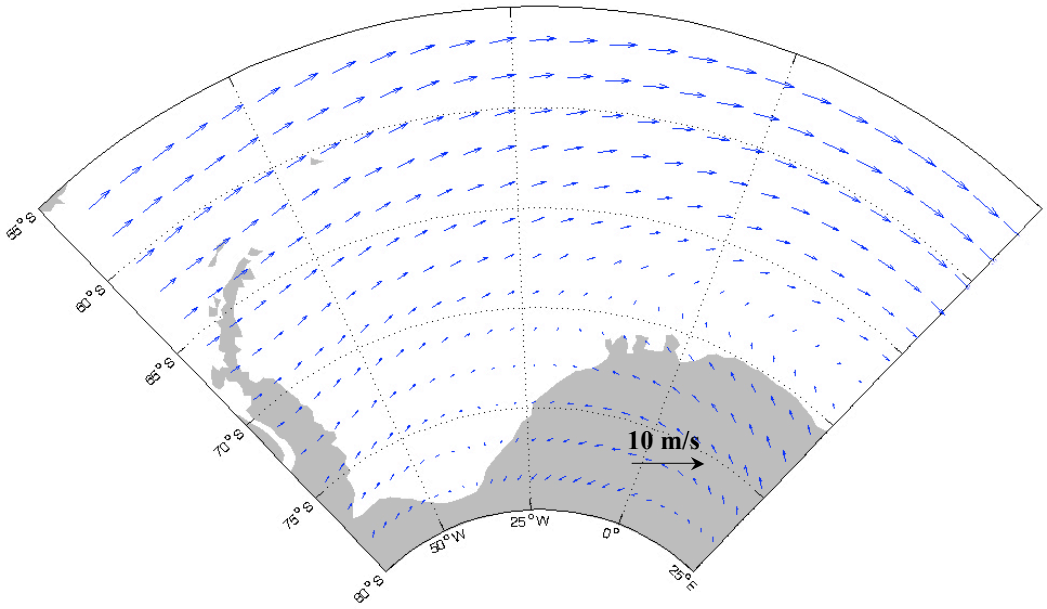

Figure 10: Annually averaged NCEP 10 m winds

In all simulation scenarios it was assumed that the entire Ronne-Filchner ice shelf collapsed instantaneously. Four scenarios were simulated to include icebergs with the following initial distributions:

1) A volume of 2.1×10^{14} m^3, corresponding to the approximate volume of the Ronne-Filchner ice shelf, was normally distributed between all eight size categories (Figure 11). With this distribution, the number of cylinders initially in each category decreases exponentially with increasing size (Figure 12), which compares well to observed distributions under normal ablative conditions (Morgan and Budd, 1978; Weeks and Mellor, 1978; Dowdeswell et al., 1992). The simulation hereinafter will be referred to as simulation "Normal".
2) The volume of the Ronne-Filchner ice shelf was initialized entirely into the largest pre-defined size category in the iceberg model (H=1181 m, Table 1). The simulation hereinafter will be referred to as simulation "Big".
3) The volume of the Ronne-Filchner ice shelf was initialized entirely into the smallest pre-defined size category in the iceberg model (H=11 m, Table 1). The simulation hereinafter will be referred to as simulation "Small".

4) The volume of the Ronne-Filchner ice shelf was initialized entirely into the pre-defined size category that most closely matched the average thickness of the ice shelf (~ 500 m). This corresponded to size category 6 (H=458 m, Table 1). The simulation hereinafter will be referred to as simulation "Shelf".

All simulation scenarios were integrated for fifty years.

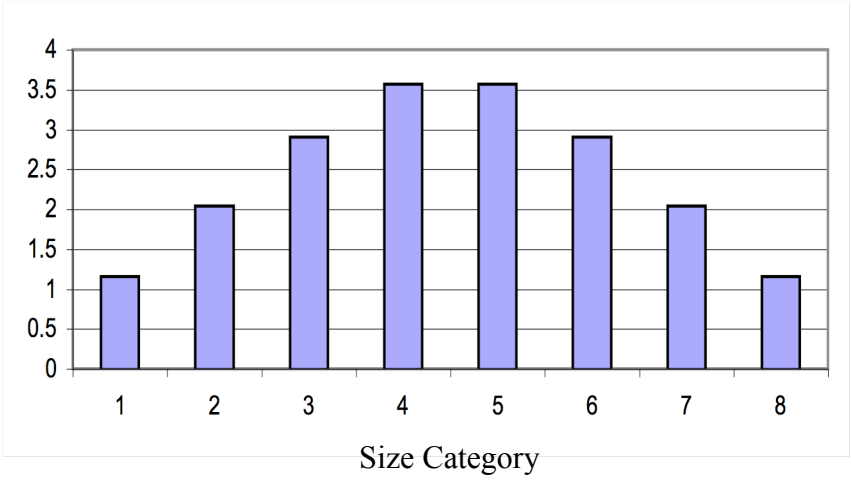

Figure 11: Simulation Normal: initial iceberg volume per size category

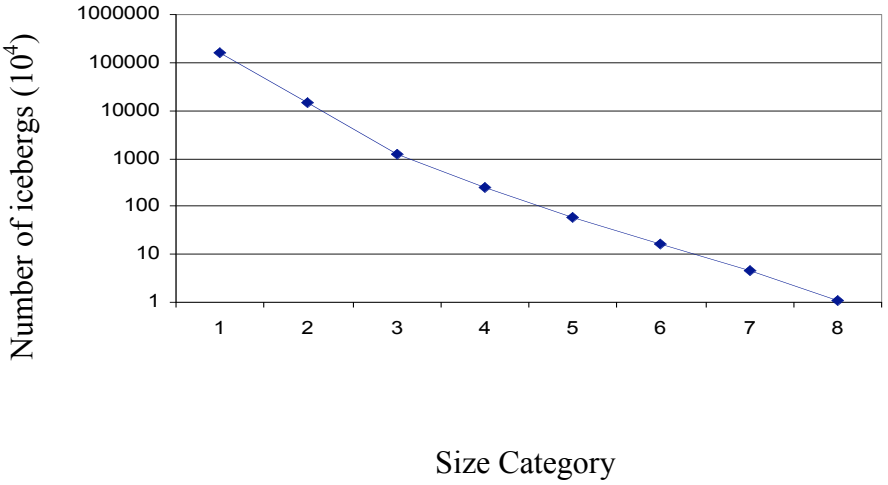

Figure 12: Simulation Normal: initial iceberg number per size category

3.3 Results and Discussion

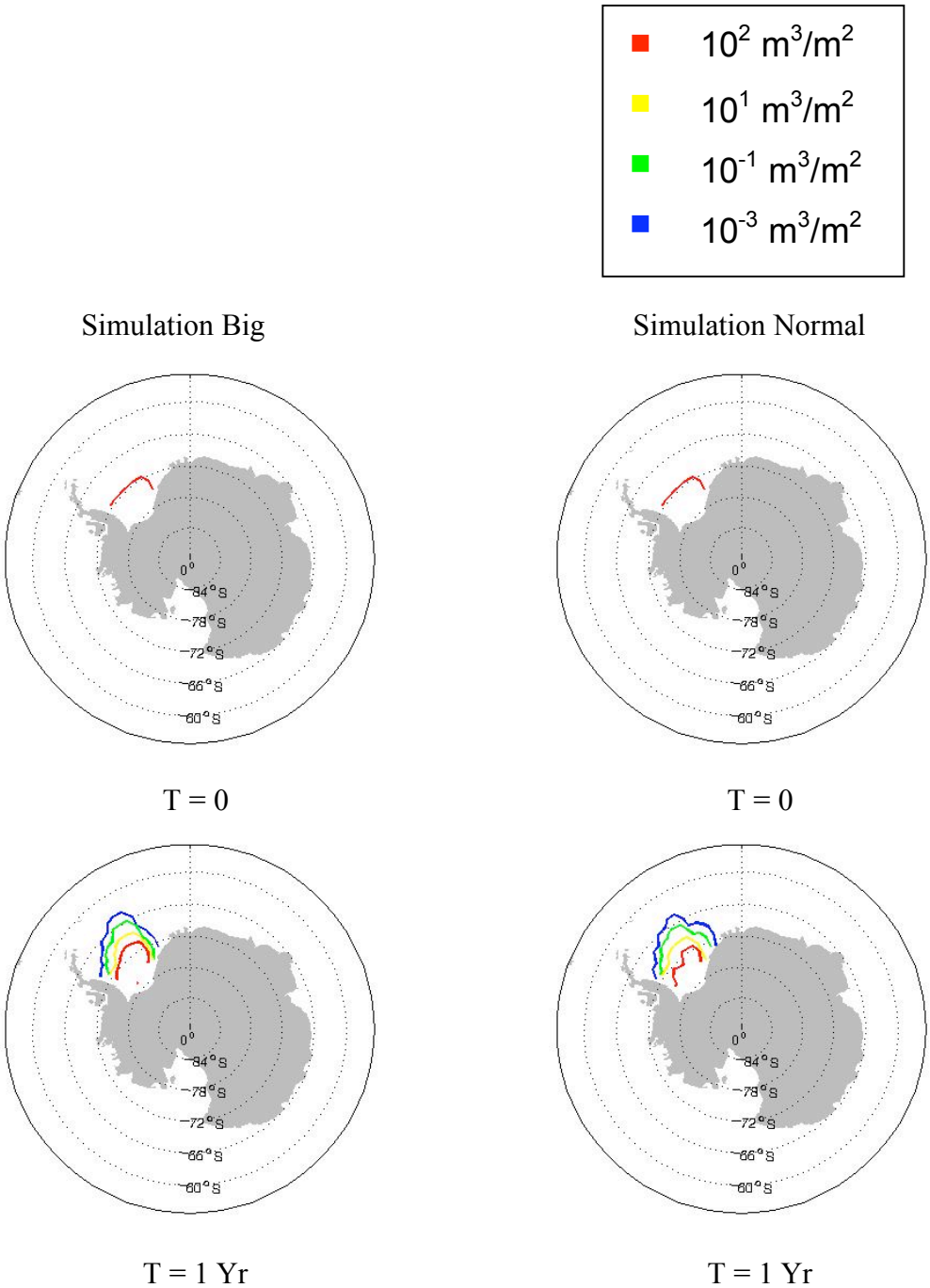

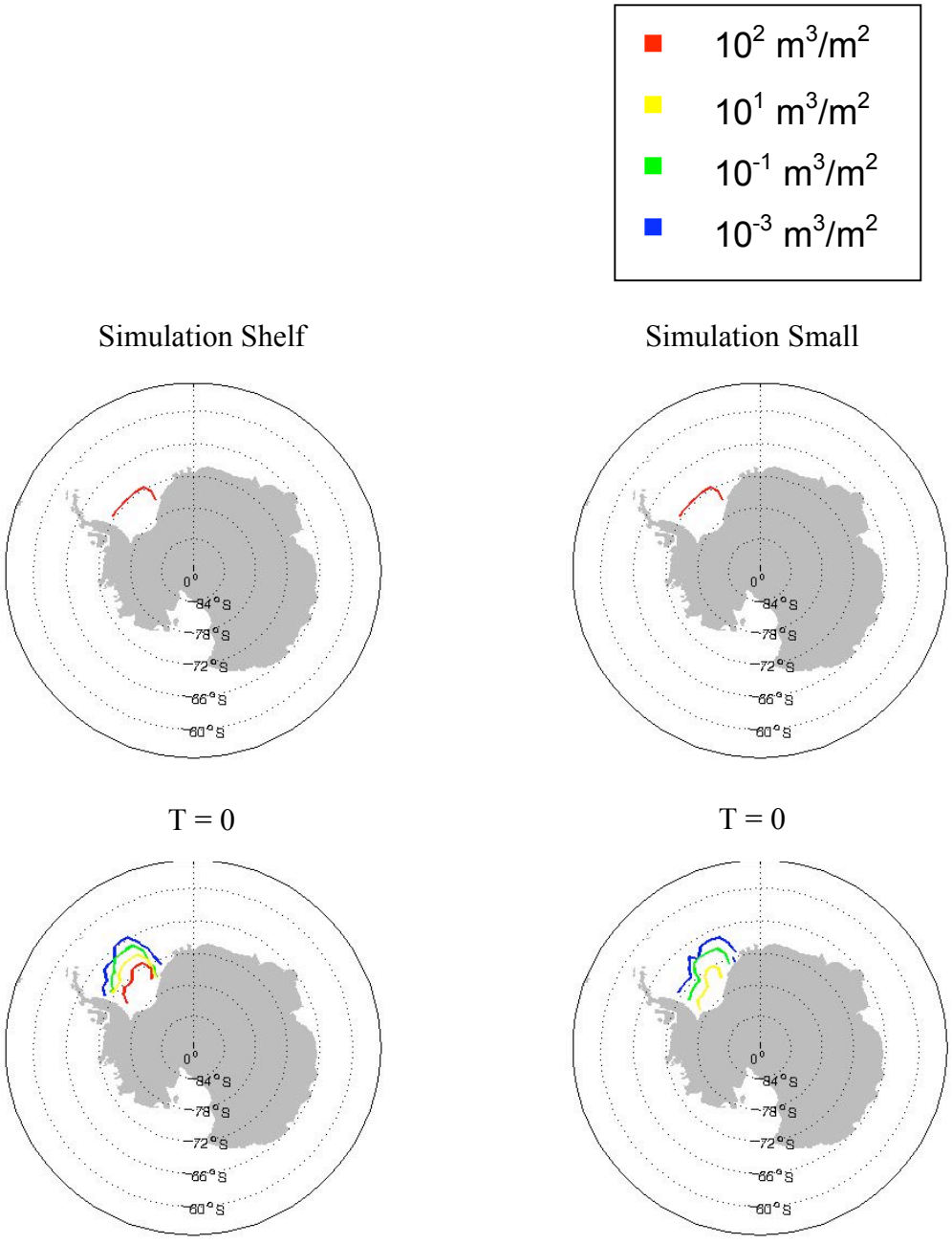
10^2 m^3/m^2
10^1 m^3/m^2
10^{-1} m^3/m^2
10^{-3} m^3/m^2
Simulation Shelf
Simulation Small
0°
84°S
78°S
72°S
66°S
60°S
T = 0
T = 0
T = 1 Yr
T = 1 Yr

Simulation Big

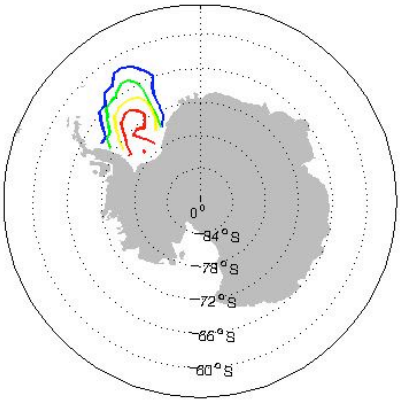

T = 3 Yr

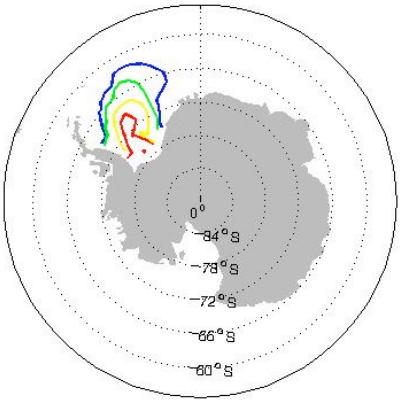

T = 5 Yr

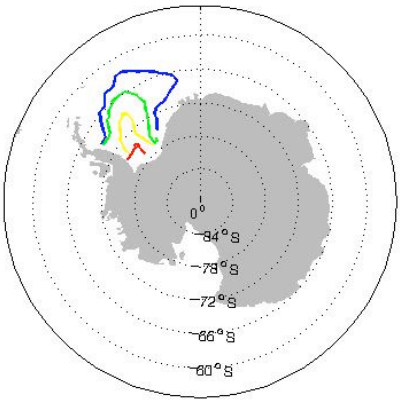

T = 10 Yr

Simulation Normal

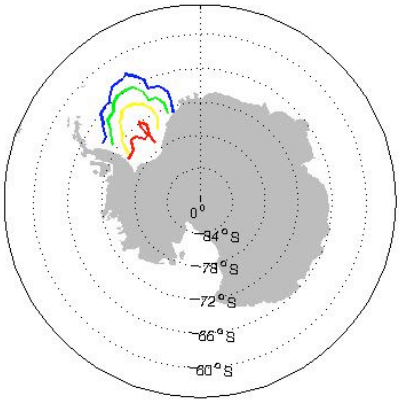

T = 3 Yr

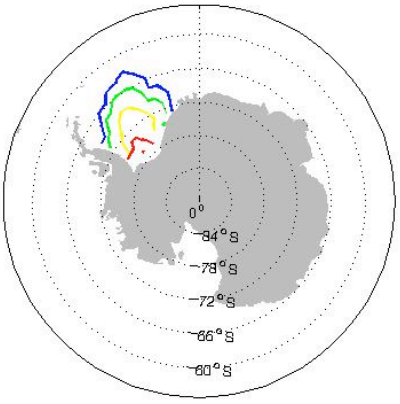

T = 5 Yr

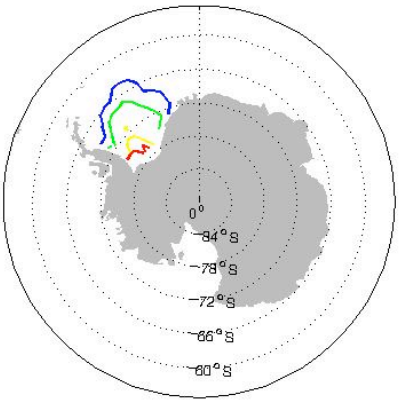

T = 10 Yr

Simulation Shelf

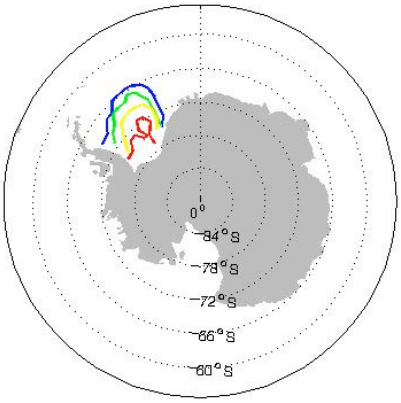

T = 3 Yr

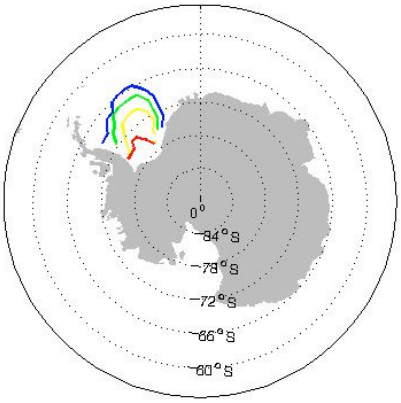

T = 5 Yr

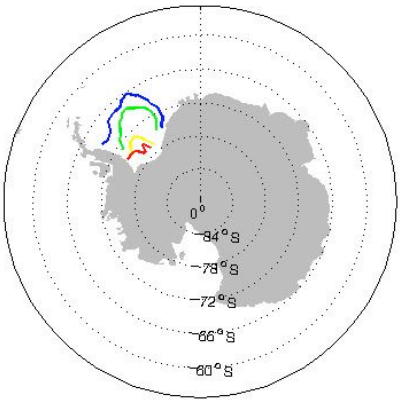

T = 10 Yr

Simulation Small

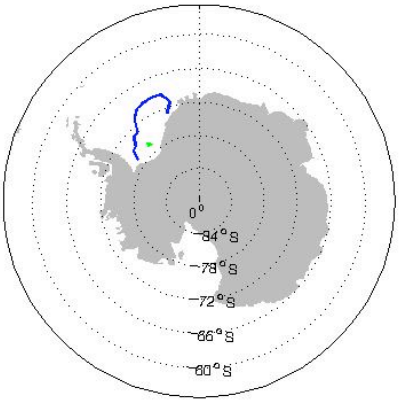

T = 3 Yr

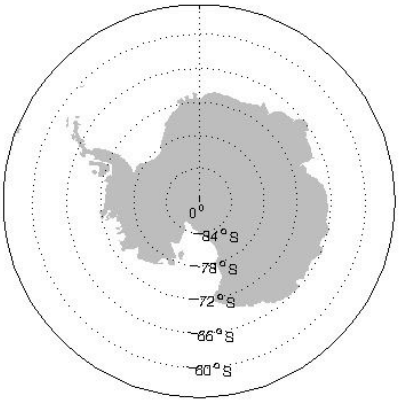

T = 5 Yr

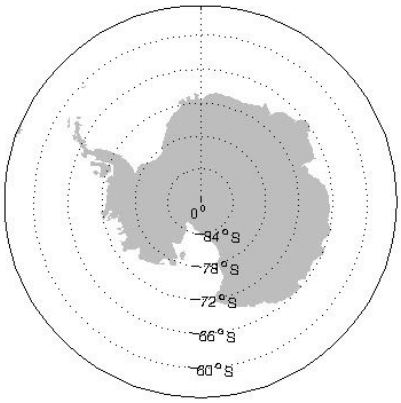

T = 10 Yr

Simulation Big

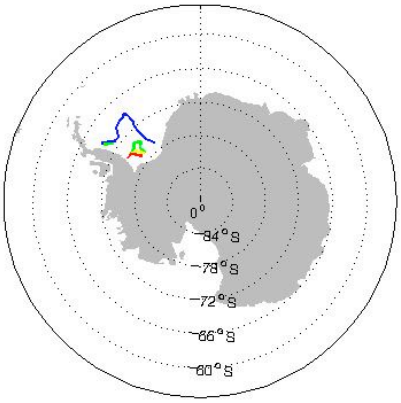

T = 25 Yr

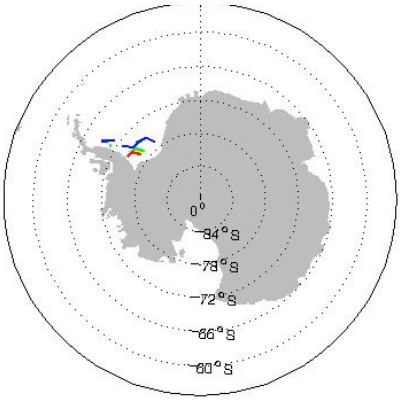

T = 50 Yr

Simulation Normal

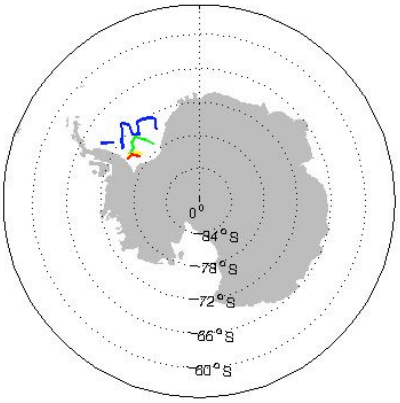

T = 25 Yr

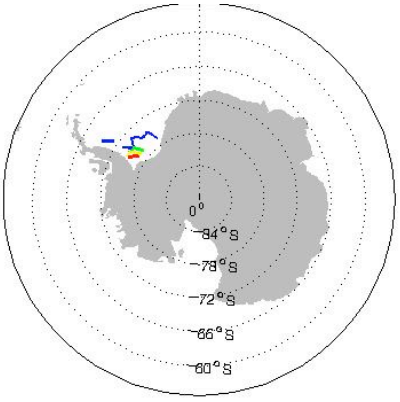

T = 50 Yr

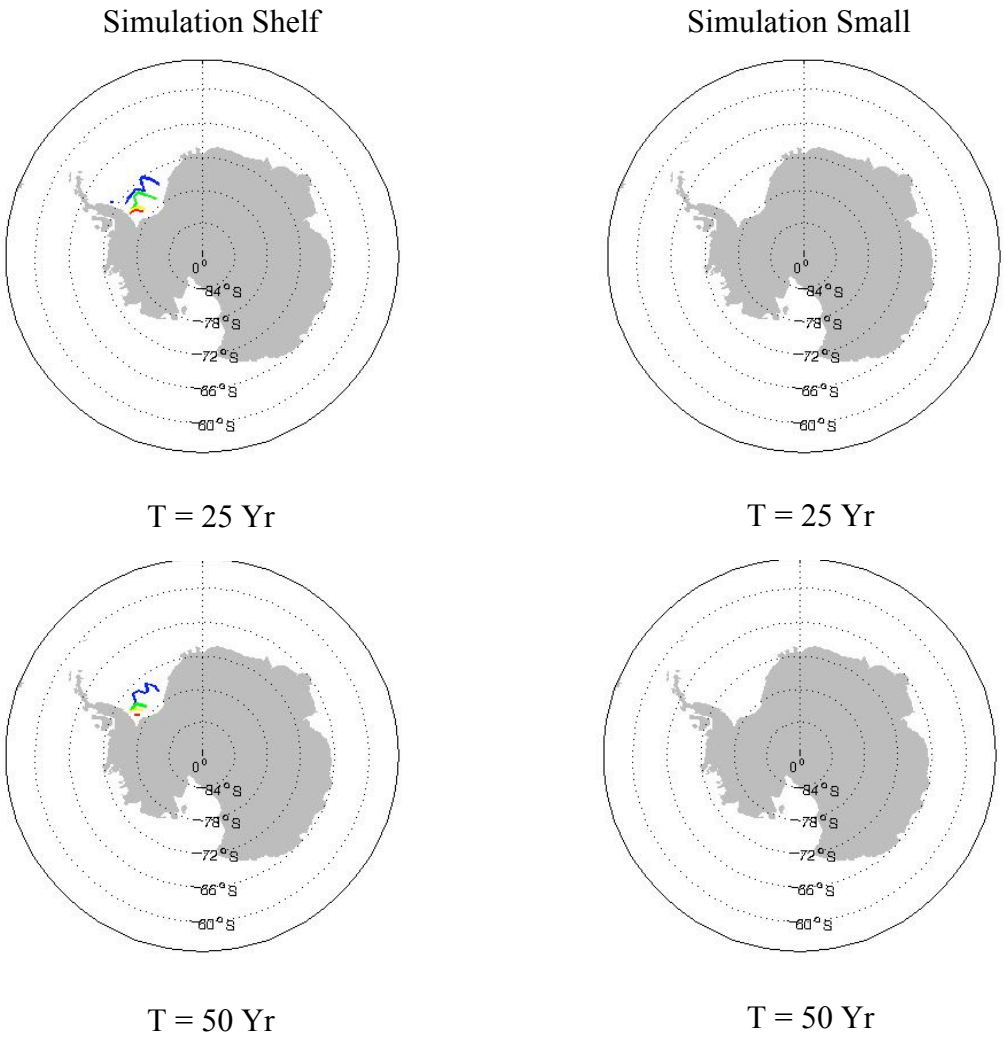

Figure 13: Total ice volume per square area at selected years after a collapse of the Ronne-Filchner ice shelf

Figure 13 shows snapshots of the total ice volume per square area of ocean surface in a logarithmic scale from the four simulations performed with the iceberg model described in chapter 2. Examining the blue 10^{-3} m^3/m^2 contours we see that some ice distributions, both in the Big and Normal simulations, reach northward to roughly 64° S within the first year. Eastward advection for the Big and Normal simulations is moderate within the first year, although, simulation Normal reaches a slightly greater eastern boundary of approximately 15° W. The Shelf simulation reaches a northern limit

of roughly 66° S and a similar eastern boundary as the Big simulation within the first year. The Small simulation shows a different behaviour than the Big simulation: on the northern front its limit spans only to roughly 68° S, but it surpasses the Big simulation on the eastern front with its limit extending to a similar boundary as simulation Normal. For all four simulations most of the icebergs are only marginally advected during the first year (red contour, 10^2 m^3/m^2).

Continuing to examine the ice distributions through time it is found that icebergs are driven by the Antarctic Circumpolar Current (ACC) once they leave the Weddell Sea. This result, as well as the overall pattern of icebergs throughout the Weddell Sea region, is complimented by observed Antarctic iceberg drift tracks throughout the Weddell Sea and surrounding area (Tchernia and Jeannin, 1984; Swithinbank et al., 1977). Examining Figure 7 through Figure 10 an increased temperature gradient, as well as dominant eastward ocean currents and winds, is found at the approximate maximum northern boundary of the ice extent for simulation Big (~ 63° S). The icebergs are therefore advected eastward to the south of this increasing temperature gradient.

In order to understand what factor was of importance in determining the northern boundary of ice distribution a sensitivity study was performed. Simulation Big was reintegrated with constant ocean temperatures of -1.7° C, named simulation "Temperature" hereinafter. It was found that the increased ocean temperatures were not primarily responsible for the northern boundary observed in simulation Big, due to the same northern boundary having been achieved in simulation Temperature (Figure 14). Therefore, the increased sea state, as a result of stronger winds, or perhaps the ocean drag must be of primary importance in determining the maximum northern boundary observed in simulation Big.

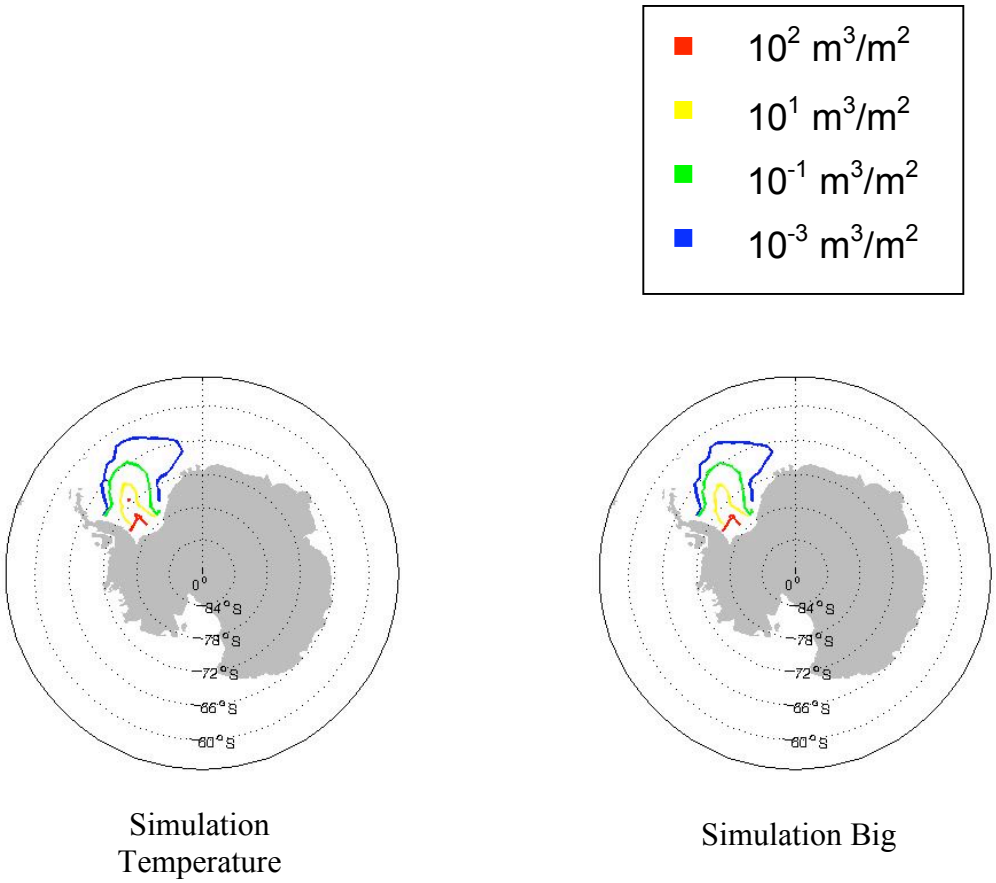

Figure 14: Total ice volume per square area at year 10 for a collapse of the Ronne-Filchner ice shelf

The Big simulation reaches maximum spatial limits of roughly 15° W and 63° S after approximately 10 years. Simulations Normal and Shelf reach their maximum spatial limits after only 5 years. The maximum spatial boundaries for simulation Normal occur at approximately 64° S and 15° W, while those for simulation Shelf are roughly located at 66° S and 20° W. The Small simulation reaches its maximum spatial extent of roughly and 66° S and 15° W after only 1 year.

After approximately 10 years, the extent of icebergs in the Big, Normal, and Shelf simulations begins to retract because local melting exceeds the advection of new icebergs into the area, and continues to do so uniformly until the end of the integrations. The ice

distribution in the Small simulation retreats rapidly compared to the other three simulations, completely melting away within the first five years.

Analyzing Figure 13, several conclusions can be drawn. Populations containing smaller icebergs are more wind-driven than those containing larger icebergs. This can be seen from the more eastward path out of the Weddell Sea that the iceberg armada follows in the Small simulation compared to the others, which become entrained in the Weddell Sea gyre. In general, large icebergs move more slowly but also melt at much slower rates (due to a lower surface area to volume ratio) than smaller icebergs. Therefore, even though the populations containing smaller icebergs take less time to reach their maximum spatial extents, they also melt at faster rates. This permits the simulations with larger icebergs to reach greater spatial expanses and decay more slowly. Also, the rapid decay of ice distribution in simulation Small indicates a substantially larger meltwater flux as compared to the other three simulations. This factor in combination with the location of deposition of the meltwater may play an important role in the stability of deep-water formation.

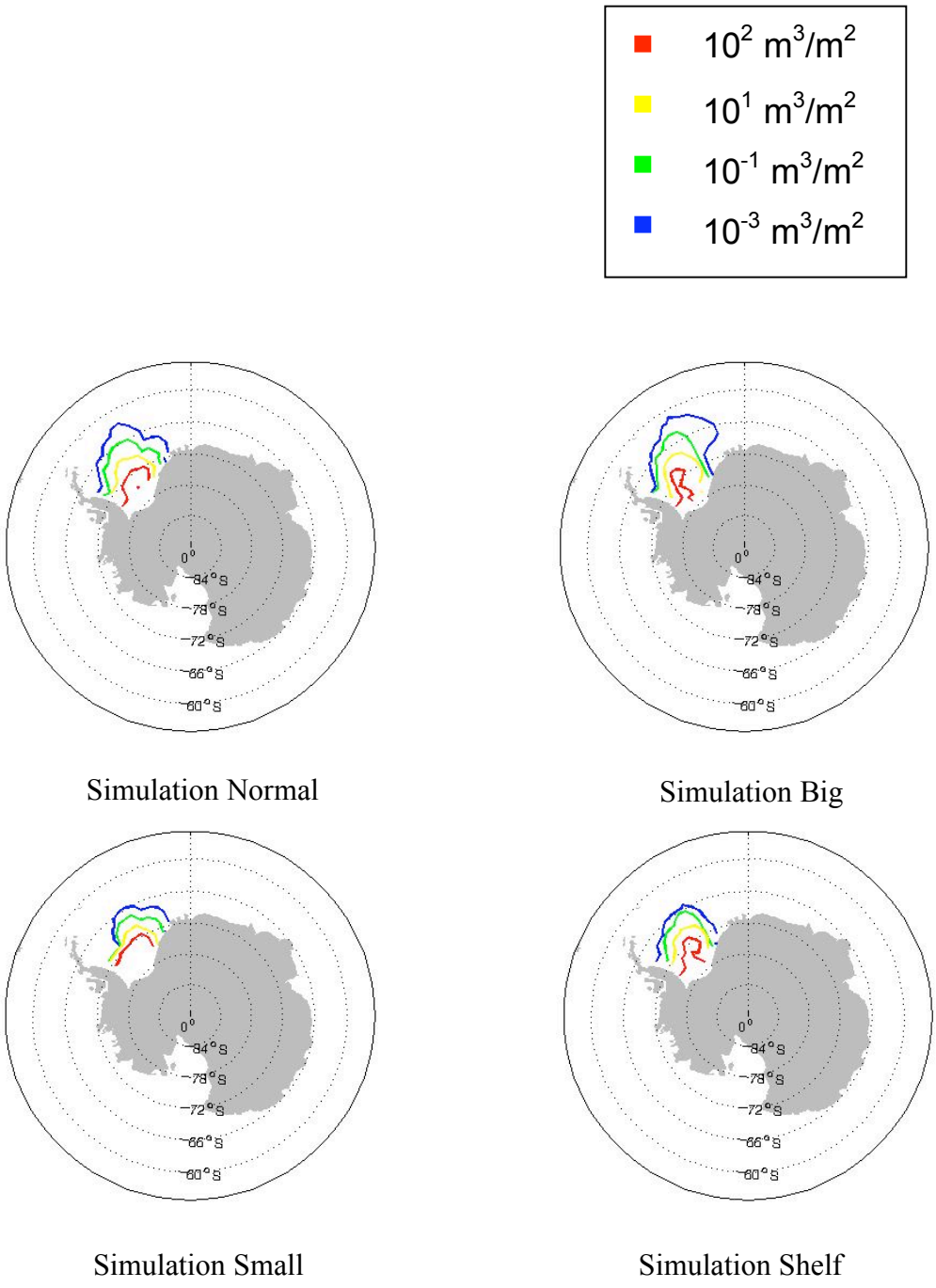

Figure 15: Total deposited meltwater volume per square area for a collapse of the Ronne-Filchner ice shelf after 50 years

The amount of total meltwater deposited throughout the fifty-year integrations is shown in Figure 15. The total deposited meltwater volume per area is contoured by the same logarithmic scale that was used for the total ice volume per area.

The Shelf and Small simulations span spatial extents more to the south compared to the Big and Normal runs. They are bounded to the north by approximately the 66° S latitude and to the east at 20° W and 15° W, respectively. Also, it is again shown that the iceberg population in the Small simulation is more wind-driven compared to the others, as can be seen by the lack of meltwater in the western Weddell Sea. Overall the meltwater distributions for the Big, Normal, and Shelf cases differ little.

The total deposited meltwater as a function of latitude for the various simulations is plotted in Figure 16 more clearly emphasizing the northern boundaries, as well as the total amount of meltwater volume that is deposited. The total deposited meltwater was integrated over 50 years for all latitude bands 1.8° in width. It can be seen, using 1 m^3 as the minimum value, that the Big and Normal simulations produce meltwater farthest north to approximately 58° S. The Small and Shelf simulations lag to the south when compared to the Big and Normal cases reaching only to roughly 63° S.

The total deposited meltwater for the simulations is also plotted as a function of longitude in Figure 17 more clearly emphasizing the eastern boundaries. The total deposited meltwater was integrated over 50 years for all longitude bands 3.6° in width. The Big simulation produces meltwater farthest to the east, again using 1 m^3 as the minimum value, at approximately 72° W. The Shelf and Normal cases produce meltwater at maximum extents of roughly 10.8° W and 50.4° W, respectively. Meltwater deposited from simulation Small only extends to approximately 3.6° W. From Figures 16 and 17 it is again clear that armadas containing smaller icebergs melt closer to the original shelf location than those containing larger icebergs.

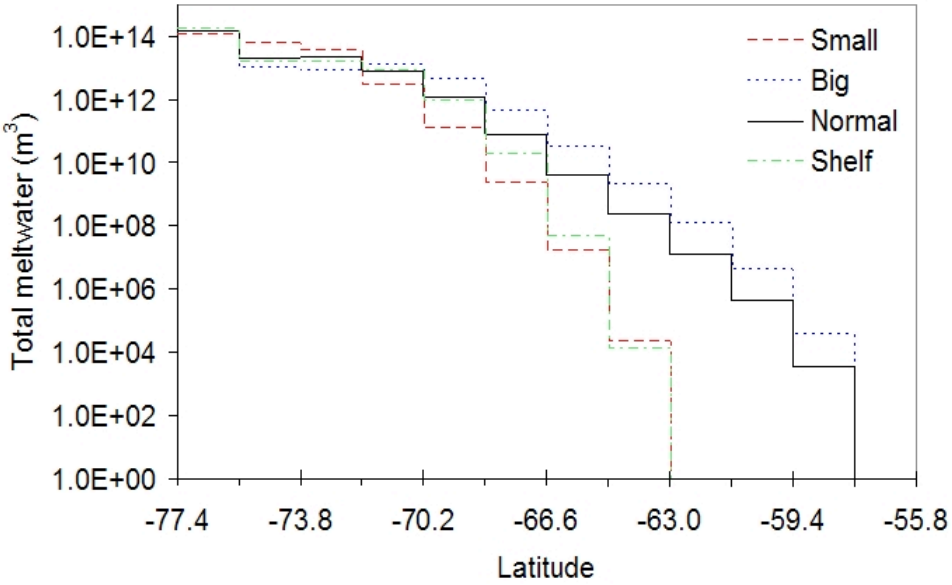

Figure 16: Total deposited meltwater volume integrated over 50 years for each latitude band 1.8° wide.

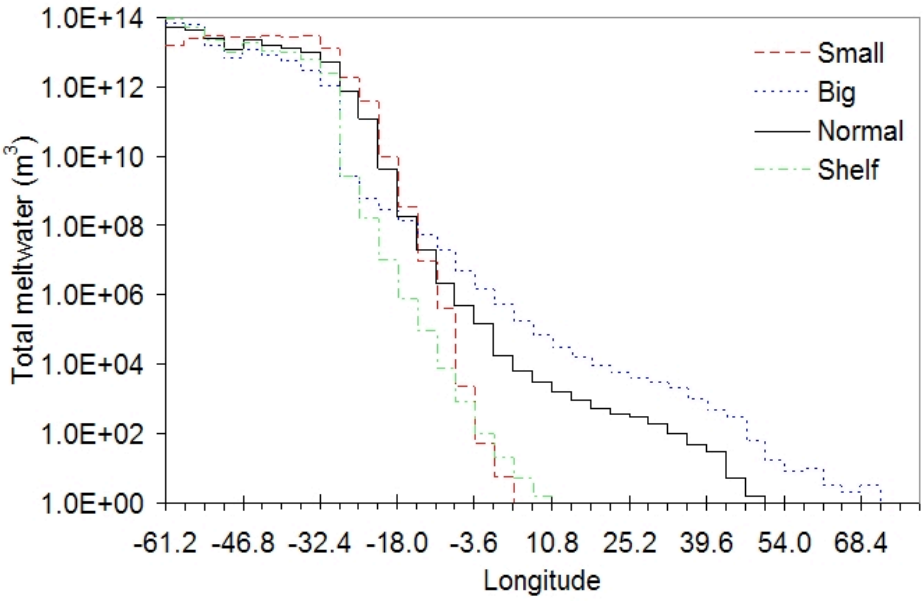

Figure 17: Total deposited meltwater volume integrated over 50 years for each longitude band 3.6° wide.

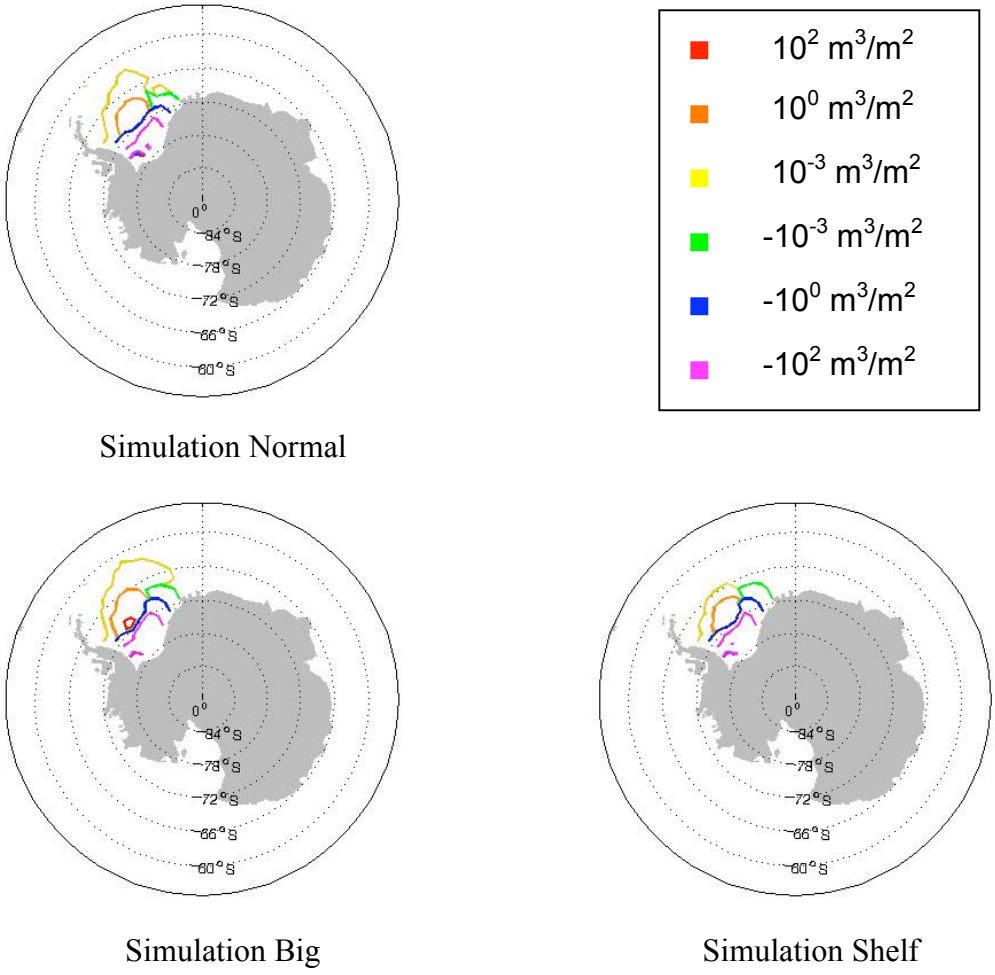

Figure 18: Total deposited meltwater volume per square area anomalies at year 50 for a collapse of the Ronne-Filchner ice shelf (compared to simulation Small)

Figure 18 shows the anomaly in total deposited meltwater for each simulation when compared to the Small simulation. It can be seen from Figure 18 that the total meltwater deposited in all simulations with respect to the Small simulation is farther from the original shelf location. Figure 18, in combination with Figure 13, clearly emphasizes the fact that populations containing smaller icebergs melt at faster rates, which correspondingly results in meltwater being deposited proximal to the original shelf location. This faster rate of melting offsets the faster speed of smaller icebergs.

The global meltwater fluxes for each of the four main cases (Normal, Big, Small, and Shelf) are plotted in Figure 19. As was shown implicitly in the total advected ice

volume per square area plots (Figure 13), the largest meltwater flux is produced with simulation Small. This is due to the fact that the total initial ice volume melts away completely within the first five years. Simulation Small produces a global meltwater flux much greater than any of the other cases with a maximum flux of 6.5 Sv initially, which declines abruptly to zero by year 3. The other three cases (Normal, Big, and Shelf) produce exponentially decreasing global meltwater fluxes; however the declines are less abrupt than that of simulation Small. Simulation Normal produces a maximum global flux of roughly 1.5 Sv initially, whereas simulations Big and Shelf produce a maximum global flux of 0.25 Sv and 0.57 Sv, respectively. The high rate of freshwater input produced in simulation Small, in combination with the flux being applied in relative close proximity to deep water formation sites, may lead to more adverse effects to the rate of deepwater formation, as compared to the other cases.

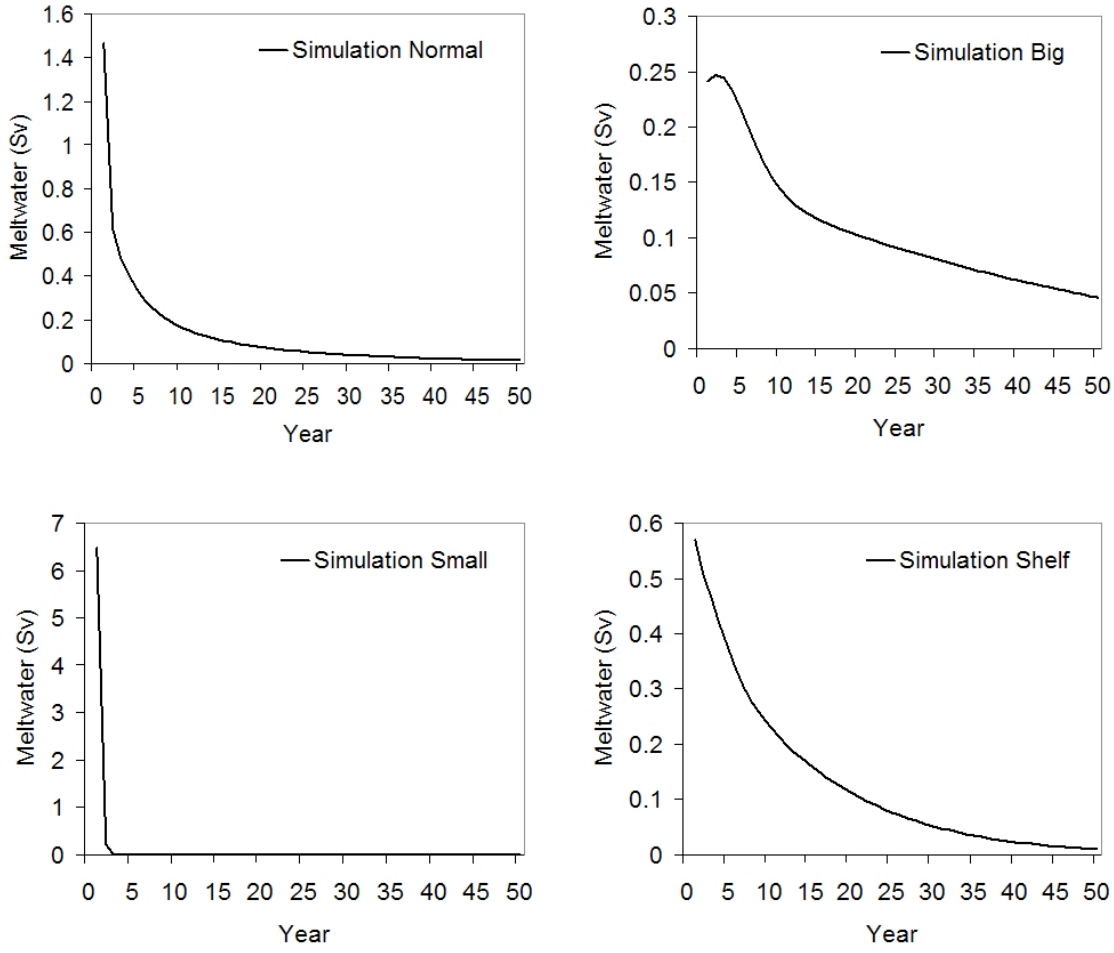

Figure 19: Global meltwater fluxes in Sverdrup (10^6 m^3s^{-1}) for various initial size distributions for a collapse of the Ronne-Filchner ice shelf. Note the different meltwater flux scales for each case.

3.4 Uncertainties

Several uncertainties and limitations of the presented simulations should be noted. The iceberg model is a standalone version driven by external forcing data; therefore, no climate feedbacks are included. As icebergs melt, they effectively cool the surrounding water and provide a freshwater source. These factors would surely affect the rates at which icebergs melt and also, possibly on longer timescales, alter ocean circulation

leading to feedbacks on the formation of icebergs. Also, the change in surface albedo due to the presence of icebergs is not modelled and there are no atmospheric feedbacks.

As was mentioned in section 3.2, environmental forcing data utilized for the present study included monthly averages for both atmospheric and oceanic fields. These data tend to smooth small temporal and spatial mesoscale features such as eddies and storms. These features could have important consequences in regards to an increase in the rate of melting, as well as the offshore advection of icebergs.

Three empirical formulas were used to represent the overall melting of icebergs in the model, the most important being wave erosion. The empirical parameterization of melting due to wave erosion in this model assumes that waves acting on icebergs are the result of local winds at the present time. This statement neglects the fact that waves present in a certain locality are most likely the result of disturbances generated a great distance away, as well as at a past time. Also, monthly averaged winds are used to define the sea state, which results in an underestimation of storms and high seas.

In order to examine the importance of the wave erosion function within the iceberg model, another sensitivity experiment was run in conjunction with the above-described simulations of chapter 3. Two simulations were integrated, one with the sea state set to stormy everywhere throughout the simulation (hereinafter referred to as simulation "Stormy", $S_s = 10$, Equation (5)), and the other with the sea state set to flat everywhere throughout the integration (hereinafter referred to as simulation "Flat", $S_s = 0$, Equation (5)). The Big simulation, which allows for variable sea states, was used as a reference. The sensitivity simulations were integrated for fifty years and were subject to the same initializations and forcings as the Big simulation.

The amounts of total deposited meltwater from the simulations were plotted as differences with respect to the Big simulation and are shown in Figure 20. In the Stormy simulation no meltwater is produced outside the Weddell Sea, whereas in the Flat simulation icebergs survive much more distal to the original shelf location as compared to simulation Big. Positive values are present and farther from the original location of the shelf but are outside the range of the scale presented. Thus, I infer the wave erosion term to be of great importance and caution must be used when implementing a function in regards to the simulated melting of icebergs due to the effects of waves.

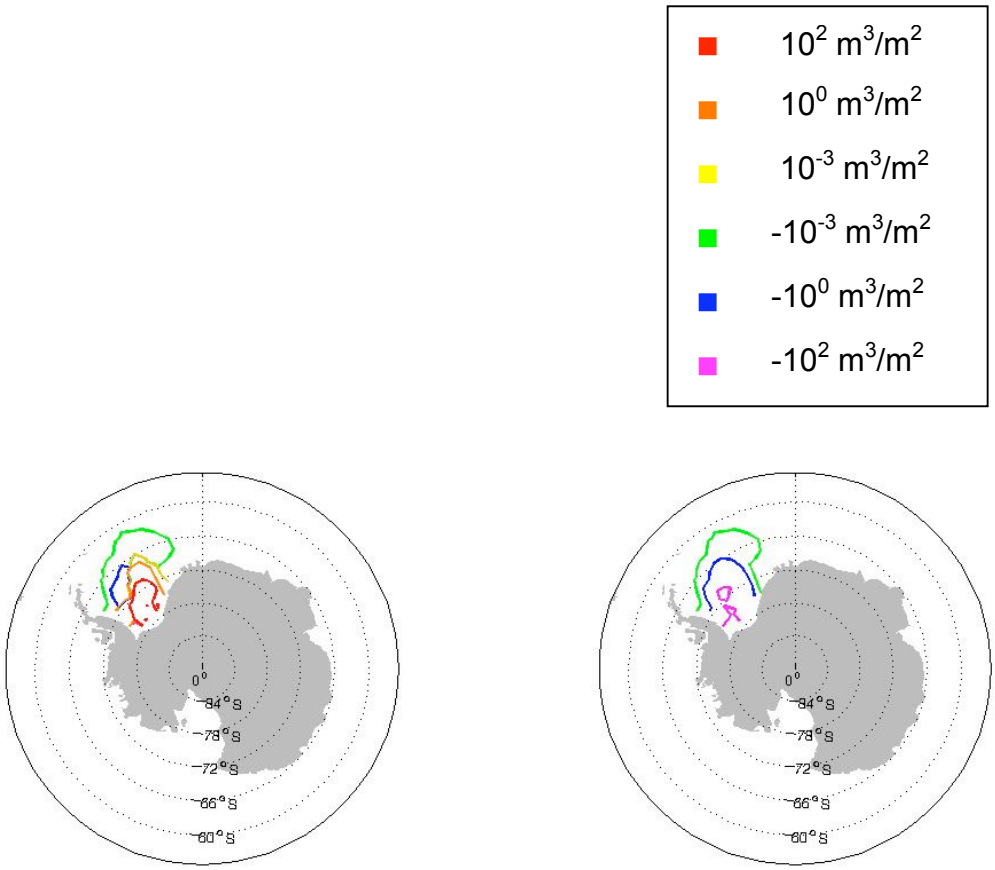

Figure 20: Total deposited meltwater volume per square area anomalies at year 50 under two extreme sea state conditions (compared to simulation Big)

The empirical function representing the melting due to basal convection at the base of the iceberg should also be mentioned. This function relates the sea surface temperature to the amount of melting taking place at the base of the iceberg, instead of taking the actual ocean temperature at the base of the iceberg into account. This approximation may, amongst other things, neglect the depression of the freezing temperature with depth, which would affect the overall melting due to basal convection over the iceberg base (Foldvik and Kvinge, 1974). A reason for this approximation is the fact that the original work of Weeks and Campbell (1973) based estimates of the basal melting rate on the available data, which included only the ocean temperatures at 20 m and those at the surface.

Several other factors important to the melting and advection of iceberg are also not incorporated in the model. Such factors include the effects due to sea ice, which may contribute significantly to overall iceberg and meltwater distributions throughout the Weddell Sea due to the abundance of sea ice cover during the winter months (NSIDC, 2009). In particular, sea ice can effectively steer icebergs, as well as protect them against the abrasive forces of waves and mitigate temperature gradients at the lateral walls (Robe, 1980). As well, the increased melting due to the effects of iceberg fracturing and rollover are not simulated in the current iceberg model.

Finally, representing the physical drift of icebergs that have the form of perfect cylinders in an environment where most icebergs resemble tabular boxes is questionable. The more tabular shape, as compared to that of a cylinder, may result in icebergs being driven proportionally more by wind than by ocean velocities.

4.0 Conclusions

4.1 Key Findings

The current study has shown that the overall distribution of icebergs, as well as their resulting meltwater locations and rates, is sensitive to their initial size distribution. Reasons for this include the surface area to volume ratio of the iceberg population, as well as the ocean and air drags the iceberg population is subjected to.

Iceberg keel depth determines the degree to which an iceberg will be driven by ocean currents. In the case of smaller icebergs, keel depth is shallow, which permits wind action to have an increased effect relative to larger icebergs. In the present study, the wind effects on populations containing greater amounts of smaller icebergs cause these armadas to follow a more eastward trajectory out of the Weddell Sea. This factor allows populations containing smaller icebergs to spend less time during the earlier part of their histories near the coast and in the vicinity of the parent ice shelf, as compared to populations containing larger icebergs.

Taking the factors above into account implies that populations containing greater amounts of smaller icebergs would achieve more expansive spatial distributions. The current study found this not to be the case. Armadas containing higher amounts of small icebergs will have greater surface area to volume ratios compared to armadas with higher amounts of large icebergs. As the energy associated with the melting of icebergs acts upon their surface area, populations containing smaller icebergs melt at a faster rate than those with larger icebergs. This increased rate of melting outweighs the effects of a more rapid wind-driven path, and causes smaller iceberg containing populations to have much more proximal spatial ice and meltwater distributions relative to the parent ice shelf. Also, populations containing smaller icebergs lead to greater meltwater fluxes due to their rapid deterioration, as compared to populations containing larger icebergs (Figure 19).

Depending on the rate and the location, meltwater from icebergs could weaken or even inhibit the formation of Antarctic Bottom Water (AABW). The present study shows

that the impact of a potential collapse of the Ronne-Filchner ice shelf on climate could depend on the size distribution of the initially generated icebergs. This is due to the variation in meltwater rate and distribution, and thus possible freshwater forcing, with initial size distribution of the icebergs. More specifically, Weddell Sea Bottom Water (WSBW), a precursor to AABW, predominantly forms over the continental shelf within the Weddell Sea. A reasonable speculation may be that initial iceberg size distributions leading to abundances of meltwater closer to the continental shelf and deposited at greater rates might have more adverse effects to WSBW formation than those producing meltwater patterns farther from the shelf and deposited at lower rates. In the present study, the iceberg population with the highest surface area to volume ratio produces a meltwater distribution closest, and at the highest rate, to the continental shelf and thus closest to the sites of WSBW formation.

4.2 Future Directions

The criticisms of section 3.4 suggest several possible avenues of research for future iceberg models. In order to investigate the climatic feedbacks associated with the advection and melting of icebergs, it is necessary to couple a dynamic-thermodynamic iceberg model to a model capable of simulating oceanic and atmospheric flows. The coupling of a sea ice component to the iceberg model is also a possibility. This would aid in the exploration of sea ice effects to the advection and melting of icebergs, as well as improve the overall simulation of iceberg dynamics and thermodynamics.

Modifications to the current functions representing the melting of icebergs offer further possible alterations. As was noted earlier, both empirical functions representing the erosion due to waves and basal convection may be over simplified. Therefore, improved representations of the factors leading to the overall melting of an iceberg could vastly enhance future iceberg simulations. Allowing modelled icebergs to fracture, as well as roll, characterize two additional features that may have positive effects to the overall accuracy when modelling icebergs. Taking these considerations into account will hopefully offer suggestions towards future studies involving the modelling of icebergs.

Bibliography

Arrigo KR, van Dijken GL, Ainley DG, Fahnesstock MA, Markus T. 2002. Ecological impact of a large Antarctic iceberg. *Geophysical Research Letters*. 29(7); p. 1104.

Beer T. 1997. *Environmental Oceanography, 2nd ed. New York:* CRC Press; 367 p.

Benn DI, Warren CR, Mottram RH. 2007. Calving processes and the dynamics of calving glaciers. *Earth-Science Reviews*. 82; pp. 143-179.

Bigg GR, Wadley MR, Stevens DP, Johnson JA. 1996. Prediction of iceberg trajectories for the North Atlantic and Arctic Oceans. *Geophysical Research Letters*. 23(24); pp. 3587-3590.

Bigg GR, Wadley MR, Stevens DP, Johnson JA. 1997. Modelling the dynamics and thermodynamics of icebergs. *Cold Regions Science and Technology*. 26; pp. 113-135.

Bond G, Broecker W, Johnsen S, McManus J, Labeyrie L, Jouzel J, Bonani G. 1993. Correlations between climate records from North-Atlantic sediments and Greenland ice. *Nature*. 365(6442); pp. 143-147.

British Antarctic Survey (BAS). 2009. <http://www.antarctica.ac.uk> Accessed 2009 Mar. 23.

Broecker WS. 1994. Massive iceberg discharges as triggers for global climate change. *Nature*. 372; pp. 421-424.

Brown CS, Sikonia WG, Post A, Rasmussen LA, Meier MF. 1983. Two calving laws for grounded iceberg-calving glaciers [Abstract]. *Annals of Glaciology*. 4; 295 p.

Clarke GKC, La Prairie DI. 2001. Modelling Iceberg Drift and Ice-Rafted Sedimentation. In: Straughan B, Greve R, Ehrentraut H, Wang Y, editors. *Continuum Mechanics and Applications in Geophysics and the Environment.* Berlin: Springer-Verlag; pp. 183-200.

Cook AJ, Fox AJ, Vaughan DG, Ferrigno JG. 2005. Retreating glacier fronts on the Antarctic Peninsula over the past half-century. *Science*. 308(5721); pp. 541-544.

Domack E, Duran D, Leventer A, Ishman S, Doane S, McCallum S, Amblas D, Ring J, Gilbert R, Prentice M. 2005. Stability of the Larsen B ice shelf on the Antarctic Peninsula during the Holocene epoch. *Nature*. 436(7051); pp. 681-685.

Dowdeswell JA, Whittington RJ, Hodgkins R. 1992. The sizes, frequencies, and freeboards of East Greenland icebergs observed using ship radar and sextant. *Journal of Geophysical Research*. 97(C3); pp. 3515-3528.

Eckart ERG, Drake RM. 1959. *Heat and Mass Transfer*. New York: McGraw-Hill; 530 p.

El-Tahan M, Venkatesh S, El-Tahan H. 1987. Validation and quantitative assessment of the deterioration mechanisms of Arctic icebergs. *Journal of Offshore Mechanics and Arctic Engineering*. 109(1); pp. 102-108

Environment Canada. 2009. <http://www.ec.gc.ca> Accessed 2009 Sep. 20.

Foldvik A, Kvinge T. 1974. Conditional instability of sea water at the freezing point. *Deep-Sea Research*. 21; pp. 169-174.

Gladstone RM, Bigg GR, Nicholls KW. 2001. Iceberg trajectory modeling and meltwater injection in the Southern Ocean. *Journal of Geophysical Research*. 106(C9); pp. 19903-19915.

Grimm EC, Jacobson Jr. GL, Watts WA, Hansen BCS, Maasch KA. 1993. A 50,000-year record of climate oscillations from Florida and its temporal correlation with the Heinrich events. *Science*. 261; pp. 198-200.

Heinrich H. 1988. Origin and consequences of cyclic ice rafting in the northeast Atlantic-ocean during the past 130,000 years. *Quaternary Research*. 29(2); pp. 142-152.

Huppert HE, Josberger EG. 1980. The melting of ice in cold stratified water. *Journal of Physical Oceanography*. 10; pp. 953-960.

Huppert HE, Turner JS. 1978. On melting icebergs. *Nature*. 271; pp. 46-48.

Jacobs SS, Helmer HH, Doake CSM, Jenkins A, Frolich RM. 1992. Melting of ice shelves and the mass balance of Antarctica. *Journal of Glaciology*. 38(130); pp. 375-387.

Jongma JI, Driesschaert E, Fichefet T, Goosse H, Renssen H. 2009. The effect of dynamic-thermodynamic icebergs on the Southern Ocean climate in a three-dimensional model. *Ocean Modelling*. 26; pp. 104-113.

Josberger EG, Neshyba S. 1980. Iceberg melt-driven convection inferred from field measurements of temperature. *Annals of Glaciology*. 1; pp. 113-117.

Kalnay E, Kanamitsu M, Kistler R, Collins W, Deaven D, Gandin L, Iredell M, Saha S, White G, Wollen J, Zhu Y, Leetmaa A, Reynolds R. 1996. The NCEP/NCAR 40

year reanalysis project. *Bulletin of the American Meterological Society*. 77; pp. 437-471.

Kundu PK, Cohen IM. 2004. *Fluid Mechanics, 3rd ed.* San Diego: Elsevier Inc.; 759 p.

La Prairie DI. 1999. *Investigating Heinrich Events: A Continuum Model of Iceberg Drift and Sedimentation* [M.Sc. Thesis]. Vancouver (BC): University of British Columbia; 100 p.

Levine RC, Bigg GR. 2008. Sensitivity of the glacial ocean to Heinrich events from different iceberg sources, as modeled by a couple atmosphere-iceberg-ocean model. *Paleoceanography*. 23.

Løset S. 1993a. Numerical modelling of the temperature distribution in tabular icebergs. *Cold Regions Science and Technology*. 21; pp. 103-115.

Løset S. 1993b. Thermal energy conservation in icebergs and tracking by temperature. *Journal of Geophysical Research*. 98(C6); pp. 10001-10012.

Matsumoto K. 1996. An iceberg drift and decay model to compute the ice-rafted debris and iceberg meltwater flux: Application to the interglacial North Atlantic. *Paleoceanography*. 11(6); pp. 729-742.

Morgan VI, Budd WF. 1978. The distribution, movement and melt rates of Antarctic icebergs. In: Husseiny, AA, editor. *Proceedings of the First Conference on Iceberg Utilization for Freshwater Production*. Iowa State University; pp. 220-228.

Mountain DG. 1980. On predicting iceberg drift. *Cold Regions Science and Technology*. 1; pp. 273-282.

National Snow and Ice Data Center (NSIDC). 2009. <http://nsidc.org> Accessed 2009 Apr. 7.

Nøst OA, Østerhus S. 1998. Impact of grounded icebergs on the hydrographic conditions near the Filchner Ice Shelf, Antarctica. In: Jacobs S, Weiss R, editors. *Ocean, Ice and Atmosphere: Interactions at the Antarctic Continental Margin*. Washigton, DC: AGU.

Paterson WSB. 1994. *The physics of glaciers, 3rd ed.* Oxford: Elsevier Science Ltd; 480 p.

Pelto MS, Warren CR. 1991. Relationship between tidewater glacier calving and water depth at the calving front. *Annals of Glaciology*. 15; pp. 115-118.

Pudsey CJ, Murray JW, Appleby P, Evans J. 2006. Lee shelf history from foraminiferal evidence, Northeast Antarctic Peninsula. *Quaternary Science Reviews*. 25(17-18); pp. 2357-2379.

Rahmstorf S. 1996. On the freshwater forcing and transport of the Atlantic thermohaline circulation. *Climate Dynamics*. 12; pp. 799-811.

Rahmstorf S. 2002. Ocean circulation and climate during the past 120,000 years. *Nature*. 419; pp. 207-214.

Reeh N. 1968. On the calving of ice from floating glaciers and ice shelves. *Journal of Glaciology*. 7; pp. 215-232.

Robe RQ. 1980. Iceberg drift and deterioration. In: Colbeck, SC, editor. *Dynamics of Snow and Ice Masses*. New York: Academic Press; pp. 211-257.

Russell-Head DS. 1980. The melting of free-drifting icebergs. *Annals of Glaciology*. 1; pp. 119-122.

Schodlok MP, Hellmer HH, Rohardt G, Fahrbach E. 2006. Weddell Sea iceberg drift: Five years of observations. *Journal of Geophysical Research*. 11.

Silva TAM, Bigg GR, Nicholls KW. 2006. Contribution of giant icebergs to the Southern Ocean freshwater flux. *Journal of Geophysical Research*. 111.

Smith SD. 1993. Hindcasting iceberg drift using current profiles and winds. *Cold Regions Science and Technology*. 22; pp. 33-45.

Sodhi DS, El-Tahan M. 1980. Prediction of an iceberg drift trajectory during a storm. *Annals of Glaciology*. 1; pp. 77-82.

Stouffer RJ, Yin J, Gregory JM, Dixon Kw, Spelman MJ, Hurlin W, Weaver AJ, Eby M, Flato GM, Hasumi H, Hu A, Jungclaus JH, Kamenkovich IV, Levermann A, Montoya M, Murakami S, Nawrath S, Oka A, Peltier WR, Robitaille DY, Sokolov A, Vettoretti G, Weber SL. 2006. Investigating the causes of the response of the thermohaline circulation to past and future climate changes. *Journal of Climate*. 19; pp. 1365-1387.

Swithinbank C, McClain P, Little P. 1977. Drift tracks of Antarctic icebergs. *Polar Record*. 18(116); pp. 495-501.

Tchernia P, Jeannin PF. 1984. Circulation in Antarctic waters as revealed by iceberg tracks. *Polar Record*. 22; pp. 263-269.

Toggweiler JR. 1994. The ocean's overturning circulation. *Physics Today*. *Nov.*; pp. 45-50.

Trenberth KE, Olson JG, Large WG. 1989. A global ocean wind stress climatology based on ECMWF analyses. *Tech. Note* NCAR/TN-338+STR, National Center for Atmospheric Research, Boulder, Co.

United States Coast Guard (USCG), International Ice Patrol (IIP). 2008. <http://www.uscg-iip.org> Accessed 2008 Sept. 20.

Van der Veen CJ. 1996. Tidewater calving. *Journal of Glaciology*. 42; pp. 375-385.

Warren CR, Kirkbride MP. 2003. Calving speed and climatic sensitivity of New Zealand lake-calving glaciers. *Annals of Glaciology*. 36; pp. 173-178.

Weaver AJ, Eby M, Wiebe EC, Bitz CM, Duffy PB, Ewen TL, Fanning AF, Holland MM, MacFadyen A, Matthews HD, Meissner KJ, Saenko O, Schmittner A, Wang H, Yoshimori M. 2001. The UVic Earth System Climate Model: model description, climatology, and applications to past, present and future climates. *Atmosphere-Ocean*. 39(4); pp. 361-428.

Weeks WF, Campbell WJ. 1973. Icebergs as a fresh-water source: an appraisal. *Journal of Glaciology*. 12(65); pp. 207-233.

Weeks WF, Mellor M. 1978. Some elements of iceberg technology. In: Husseiny AA, editor. *Proceedings of the First Conference on Iceberg Utilization for Freshwater Production*. Iowa State University, pp. 45-98.